7. Lassmann H, van Horssen J. The molecular basis of neurodegeneration in multiple sclerosis. *FEBS Lett*. 2011; **585**: 3715–23.
8. Popescu BF, Lucchinetti CF. Pathology of demyelinating diseases. *Annu Rev Pathol*. 2012; **7**: 185–217.
9. Gandhi R, Laroni A, Weiner HL. Role of the innate immune system in the pathogenesis of multiple sclerosis. *J Neuroimmunol*. 2010; **221**: 7–14.
10. Mayo L, Quintana FJ, Weiner HL. The innate immune system in demyelinating disease. *Immunol Rev*. 2012; **248**: 170–87.
11. Haghikia A, Hohlfeld R, Gold R, Fugger L. Therapies for multiple sclerosis: translational achievements and outstanding needs. *Trends Mol Med*. 2013; **19**: 309–19.
12. Braley TJ, Segal BM. B-cell targeting agents in the treatment of multiple sclerosis. *Curr Treat Options Neurol*. 2013; **15**: 259–69.
13. Gergely P, Nuesslein-Hildesheim B, Guerini D, et al. The selective sphingosine 1-phosphate receptor modulator BAF312 redirects lymphocyte distribution and has species-specific effects on heart rate. *Br J Pharmacol*. 2012; **167**: 1035–47.
14. Fujita T, Inoue K, Yamamoto S, et al. Fungal metabolites. Part 11. A potent immunosuppressive activity found in Isaria sinclairii metabolite. *J Antibiot (Tokyo)*. 1994; **47**: 208–15.
15. Kapoor R, Furby J, Hayton T, et al. Lamotrigine for neuroprotection in secondary progressive multiple sclerosis: a randomised, double-blind, placebo-controlled, parallel-group trial. *Lancet Neurol*. 2010; **9**: 681–8.
16. Yadav V, Marracci G, Lovera J, et al. Lipoic acid in multiple sclerosis: a pilot study. *Mult Scler*. 2005; **11**: 159–65.
17. Killestein J, Kalkers NF, Polman CH. Glutamate inhibition in MS: the neuroprotective properties of riluzole. *J Neurol Sci*. 2005; **233**: 113–5.
18. Sheremata WA, Vollmer TL, Stone LA, Willmer-Hulme AJ, Koller M. A safety and pharmacokinetic study of intravenous natalizumab in patients with MS. *Neurology*. 1999; **52**: 1072–4.
19. Coles AJ, Fox E, Vladic A, et al. Alemtuzumab versus interferon beta-1a in early relapsing-remitting multiple sclerosis: post-hoc and subset analyses of clinical efficacy outcomes. *Lancet Neurol*. 2011; **10**: 338–48.
20. Rose JW, Burns JB, Bjorklund J, Klein J, Watt HE, Carlson NG. Daclizumab phase II trial in relapsing and remitting multiple sclerosis: MRI and clinical results. *Neurology*. 2007; **69**: 785–9.
21. Buttmann M. Treating multiple sclerosis with monoclonal antibodies: a 2010 update. *Expert Rev Neurother*. 2010; **10**: 791–809.
22. Hauser SL, Waubant E, Arnold DL, et al. B-cell depletion with rituximab in relapsing-remitting multiple sclerosis. *N Engl J Med*. 2008; **358**: 676–88.
23. Edelman GM, Benacerraf B, Ovary Z, Poulik MD. Structural differences among antibodies of different specificities. *Proc Natl Acad Sci USA*. 1961; **47**: 1751–8.
24. Kohler G, Milstein C. Continuous cultures of fused cells secreting antibody of predefined specificity. *Nature*. 1975; **256**: 495–7.
25. Beck A, Haeuw JF, Wurch T, Goetsch L, Bailly C, Corvaia N. The next generation of antibody-drug conjugates comes of age. *Discov Med*. 2010; **10**: 329–39.
26. Weinshenker BG, Bass B, Karlik S, Ebers GC, Rice GP. An open trial of OKT3 in patients with multiple sclerosis. *Neurology*. 1991; **41**: 1047–52.
27. Daifotis AG, Koenig S, Chatenoud L, Herold KC. Anti-CD3 clinical trials in type 1 diabetes mellitus. *Clin Immunol*. 2013; **149**: 268–78.
28. Lindsey JW, Hodgkinson S, Mehta R, Mitchell D, Enzmann D, Steinman L. Repeated treatment with chimeric anti-CD4 antibody in multiple sclerosis. *Ann Neurol*. 1994; **36**: 183–9.
29. Lindsey JW, Hodgkinson S, Mehta R, et al. Phase 1 clinical trial of chimeric monoclonal anti-CD4 antibody in multiple sclerosis. *Neurology*. 1994; **44**: 413–9.
30. van Oosten BW, Lai M, Barkhof F, et al. A phase II trial of anti-CD4 antibodies in the treatment of multiple sclerosis. *Mult Scler*. 1996; **1**: 339–42.
31. Rep MH, van Oosten BW, Roos MT, Ader HJ, Polman CH, van Lier RA. Treatment with depleting CD4 monoclonal antibody results in a preferential loss of circulating naive T cells but does not affect IFN-gamma secreting TH1 cells in humans. *J Clin Investig*. 1997; **99**: 2225–31.
32. Klinkert WE, Kojima K, Lesslauer W, Rinner W, Lassmann H, Wekerle H. TNF-alpha receptor fusion protein prevents experimental auto-immune encephalomyelitis and demyelination in Lewis rats: an overview. *J Neuroimmunol*. 1997; **72**: 163–8.
33. van Oosten BW, Barkhof F, Truyen L, et al. Increased MRI activity and immune activation in two multiple sclerosis patients treated with the monoclonal anti-tumor necrosis factor antibody cA2. *Neurology*. 1996; **47**: 1531–4.
34. Mohan N, Edwards ET, Cupps TR, et al. Demyelination occurring during anti-tumor necrosis factor alpha therapy for inflammatory arthritides. *Arthritis Rheum*. 2001; **44**: 2862–9.
35. TNF neutralization in MS: results of a randomized, placebo-controlled multicenter study. The Lenercept Multiple Sclerosis Study Group and The University of British Columbia MS/MRI Analysis Group. *Neurology*. 1999; **53**: 457–65.
36. Kassiotis G, Kollias G. Uncoupling the proinflammatory from the immunosuppressive properties of tumor necrosis factor (TNF) at the p55 TNF receptor level: implications for pathogenesis and therapy of autoimmune demyelination. *J Exp Med*. 2001; **193**: 427–34.
37. Croxford JL, Triantaphyllopoulos KA, Neve RM, Feldmann M, Chernajovsky Y, Baker D. Gene therapy for chronic

relapsing experimental allergic encephalomyelitis using cells expressing a novel soluble p75 dimeric TNF receptor. *J Immunol*. 2000; **164**: 2776–81.
38. Sean Riminton D, Korner H, Strickland DH, Lemckert FA, Pollard JD, Sedgwick JD. Challenging cytokine redundancy: inflammatory cell movement and clinical course of experimental autoimmune encephalomyelitis are normal in lymphotoxin-deficient, but not tumor necrosis factor-deficient, mice. *J Exp Med*. 1998; **187**: 1517–28.
39. Arnett HA, Mason J, Marino M, Suzuki K, Matsushima GK, Ting JP. TNF alpha promotes proliferation of oligodendrocyte progenitors and remyelination. *Nat Neurosci*. 2001; **4**: 1116–22.
40. Faustman D, Davis M. TNF receptor 2 pathway: drug target for autoimmune diseases. *Nat Rev Drug Discovery*. 2010; **9**: 482–93.
41. Toussirot E, Michel F, Bereau M, Binda D. Ustekinumab in chronic immune-mediated diseases: a review of long term safety and patient improvement. *Patient Prefer Adherence*. 2013; **7**: 369–77.
42. Segal BM, Constantinescu CS, Raychaudhuri A, et al. Repeated subcutaneous injections of IL12/23 p40 neutralising antibody, ustekinumab, in patients with relapsing-remitting multiple sclerosis: a phase II, double-blind, placebo-controlled, randomised, dose-ranging study. *Lancet Neurol*. 2008; **7**: 796–804.
43. Thakker P, Leach MW, Kuang W, Benoit SE, Leonard JP, Marusic S. IL-23 is critical in the induction but not in the effector phase of experimental autoimmune encephalomyelitis. *J Immunol*. 2007; **178**: 2589–98.
44. Toussirot E. The IL23/Th17 pathway as a therapeutic target in chronic inflammatory diseases. *Inflamm Allergy Drug Targets*. 2012; **11**: 159–68.
45. Patel DD, Lee DM, Kolbinger F, Antoni C. Effect of IL-17A blockade with secukinumab in autoimmune diseases. *Ann Rheum Dis*. 2013; **72**(Suppl 2): ii116–23.
46. Knier B, Hemmer B, Korn T. Novel monoclonal antibodies for therapy of multiple sclerosis. *Expert Opin Biol Ther*. 2014; **14**: 503–13.
47. Riechmann L, Clark M, Waldmann H, Winter G. Reshaping human antibodies for therapy. *Nature*. 1988; **332**: 323–7.
48. Gilleece MH, Dexter TM. Effect of Campath-1H antibody on human hematopoietic progenitors *in vitro*. *Blood*. 1993; **82**: 807–12.
49. Waldmann H, Hale G. CAMPATH: from concept to clinic. *Philos Trans R Soc Lond B Biol Sci*. 2005; **360**: 1707–11.
50. Kousin-Ezewu O, Coles A. Alemtuzumab in multiple sclerosis: latest evidence and clinical prospects. *Ther Adv Chronic Dis*. 2013; **4**: 97–103.
51. Coles AJ, Wing MG, Molyneux P, et al. Monoclonal antibody treatment exposes three mechanisms underlying the clinical course of multiple sclerosis. *Ann Neurol*. 1999; **46**: 296–304.
52. Coles AJ, Cox A, Le Page E, et al. The window of therapeutic opportunity in multiple sclerosis: evidence from monoclonal antibody therapy. *J Neurol*. 2006; **253**: 98–108.
53. Investigators CT, Coles AJ, Compston DA, et al. Alemtuzumab vs. interferon beta-1a in early multiple sclerosis. *The New England journal of medicine*. 2008; **359**: 1786–801.
54. Coles AJ, Twyman CL, Arnold DL, et al. Alemtuzumab for patients with relapsing multiple sclerosis after disease-modifying therapy: a randomised controlled phase 3 trial. *Lancet*. 2012; **380**: 1829–39.
55. Cohen JA, Coles AJ, Arnold DL, et al. Alemtuzumab versus interferon beta 1a as first-line treatment for patients with relapsing-remitting multiple sclerosis: a randomised controlled phase 3 trial. *Lancet*. 2012; **380**: 1819–28.
56. Coles AJ, Fox E, Vladic A, et al. Alemtuzumab more effective than interferon beta-1a at 5-year follow-up of CAMMS223 clinical trial. *Neurology*. 2012; **78**: 1069–78.
57. Freedman MS, Kaplan JM, Markovic-Plese S. Insights into the mechanisms of the therapeutic efficacy of alemtuzumab in multiple sclerosis. *J Clin Cell Immunol*. 2013; **4**: pii: 1000152.
58. Jones JL, Anderson JM, Phuah CL, et al. Improvement in disability after alemtuzumab treatment of multiple sclerosis is associated with neuroprotective autoimmunity. *Brain*. 2010; **133**: 2232–47.
59. Malek TR. The biology of interleukin-2. *Annu Rev Immunol*. 2008; **26**: 453–79.
60. Waldmann TA. Anti-Tac (daclizumab, Zenapax) in the treatment of leukemia, autoimmune diseases, and in the prevention of allograft rejection: a 25-year personal odyssey. *J Clin Immunol*. 2007; **27**: 1–18.
61. Lin JX, Leonard WJ. Signaling from the IL-2 receptor to the nucleus. *Cytokine Growth Factor Rev*. 1997; **8**: 313–32.
62. Queen C, Schneider WP, Selick HE, et al. A humanized antibody that binds to the interleukin 2 receptor. *Proc Natl Acad Sci USA*. 1989; **86**: 10029–33.
63. Setoguchi R, Hori S, Takahashi T, Sakaguchi S. Homeostatic maintenance of natural Foxp3(+) CD25(+) CD4(+) regulatory T cells by interleukin (IL)-2 and induction of autoimmune disease by IL-2 neutralization. *J Exp Med*. 2005; **201**: 723–35.
64. Martin JF, Perry JS, Jakhete NR, Wang X, Bielekova B. An IL-2 paradox: blocking CD25 on T cells induces IL-2-driven activation of CD56(bright) NK cells. *J Immunol*. 2010; **185**: 1311–20.
65. Baan CC, Balk AH, van Riemsdijk IC, et al. Anti-CD25 monoclonal antibody therapy affects the death signals of graft-infiltrating cells after clinical heart transplantation. *Transplantation*. 2003; **75**: 1704–10.
66. Roifman CM. Human IL-2 receptor alpha chain deficiency. *Pediatr Res*. 2000; **48**: 6–11.

67. Martin R. Anti-CD25 (daclizumab) monoclonal antibody therapy in relapsing-remitting multiple sclerosis. *Clin Immunol*. 2012; **142**: 9–14.
68. Bielekova B, Richert N, Howard T, et al. Humanized anti-CD25 (daclizumab) inhibits disease activity in multiple sclerosis patients failing to respond to interferon beta. *Proc Natl Acad Sci USA*. 2004; **101**: 8705–8.
69. Bielekova B, Howard T, Packer AN, et al. Effect of anti-CD25 antibody daclizumab in the inhibition of inflammation and stabilization of disease progression in multiple sclerosis. *Arch Neurol*. 2009; **66**: 483–9.
70. Rose JW, Watt HE, White AT, Carlson NG. Treatment of multiple sclerosis with an anti-interleukin-2 receptor monoclonal antibody. *Ann Neurol*. 2004; **56**: 864–7.
71. Wynn D, Kaufman M, Montalban X, et al. Daclizumab in active relapsing multiple sclerosis (CHOICE study): a phase 2, randomised, double-blind, placebo-controlled, add-on trial with interferon beta. *Lancet Neurol*. 2010; **9**: 381–90.
72. Gold R, Giovannoni G, Selmaj K, et al. Daclizumab high-yield process in relapsing-remitting multiple sclerosis (SELECT): a randomised, double-blind, placebo-controlled trial. *Lancet*. 2013; **381**: 2167–75.
73. Bielekova B. Daclizumab therapy for multiple sclerosis. Neurotherapeutics: the journal of the American Society for Experimental. *Neurotherapeutics*. 2013; **10**: 55–67.
74. Bielekova B, Catalfamo M, Reichert-Scrivner S, et al. Regulatory CD56(bright) natural killer cells mediate immunomodulatory effects of IL-2Ralpha-targeted therapy (daclizumab) in multiple sclerosis. *Proc Natl Acad Sci USA*. 2006; **103**: 5941–6.
75. Bielekova B, Richert N, Herman ML, et al. Intrathecal effects of daclizumab treatment of multiple sclerosis. *Neurology*. 2011; **77**: 1877–86.
76. Pfender N, Martin R. Daclizumab (anti-CD25) in multiple sclerosis. *Exp Neurol*. 2014; **262**: 44–51.
77. Wuest SC, Edwan JH, Martin JF, et al. A role for interleukin-2 trans-presentation in dendritic cell-mediated T cell activation in humans, as revealed by daclizumab therapy. *Nat Med*. 2011; **17**: 604–9.

OPEN ACCESS Freely available online

PLOS | ONE

^{11}C-Acetate PET Imaging in Patients with Multiple Sclerosis

Kazushiro Takata[1☯], Hiroki Kato[2☯], Eku Shimosegawa[2], Tatsusada Okuno[1], Toru Koda[1], Tomoyuki Sugimoto[3], Hideki Mochizuki[1], Jun Hatazawa[2,4*], Yuji Nakatsuji[1*]

1 Department of Neurology, Osaka University Graduate School of Medicine, Suita, Osaka, Japan, **2** Department of Nuclear Medicine and Tracer Kinetics, Osaka University Graduate School of Medicine, Suita, Osaka, Japan, **3** Hirosaki University Graduate School of Science and Technology, Hirosaki, Aomori, Japan, **4** WPI-Immunology Frontier Research Center, Osaka University, Suita, Osaka, Japan

Abstract

Background: Activation of glial cells is a cardinal feature in multiple sclerosis (MS) pathology, and acetate has been reported to be selectively uptaken by astrocytes in the CNS. The aim of this study was to investigate the efficacy of PET with ^{11}C-acetate for MS diagnosis.

Materials and Methods: Six patients with relapsing-remitting MS and 6 healthy volunteers (HV) were enrolled. The ^{11}C-acetate brain uptake on PET was measured in patients with MS and HV. Volume-of-interest analysis of cerebral gray and white matter based on the segmentation technique for co-registered MRI and voxel-based statistical parametric analysis were performed. Correlation between ^{11}C-acetate uptake and the lesion number in T1- and T2- weighted MR images were also assessed.

Results: The standardized uptake value (SUV) of ^{11}C-acetate was increased in both white and gray matter in MS patients compared to HV. Voxel-based statistical analysis revealed a significantly increased SUV relative to that in the bilateral thalami (SUVt) in a broad area of white matter, particularly in the subcortical white matter of MS patients. The numbers of T2 lesions and T1 black holes were significantly correlated with SUV of ^{11}C-acetate in white and gray matter.

Conclusions: The ^{11}C-acetate uptake significantly increased in MS patients and correlated to the number of MRI lesions. These preliminary data suggest that ^{11}C-acetate PET can be a useful clinical examination for MS patients.

Citation: Takata K, Kato H, Shimosegawa E, Okuno T, Koda T, et al. (2014) ^{11}C-Acetate PET Imaging in Patients with Multiple Sclerosis. PLoS ONE 9(11): e111598. doi:10.1371/journal.pone.0111598

Editor: Akio Suzumura, Research Inst. of Environmental Med., Nagoya Univ., Japan

Received August 21, 2014; **Accepted** September 25, 2014; **Published** November 4, 2014

Data Availability: The authors confirm that all data underlying the findings are fully available without restriction. All relevant data are within the paper and its Supporting Information files.

Funding: This study was supported by the Health and Labor Sciences Research Grants from the Ministry of Health, Labor and Welfare of Japan, by a Grant-in-Aid for Scientific Research of Japan Society for the Promotion of Science (YN and TO) and by the Japan Society for the Promotion of Science KAKENHI Grant Number 23592089 (HK). The funders had no role in study design, data collection and analysis, decision to publish, or preparation of the manuscript.

Competing Interests: The authors have declared that no competing interests exist.

* Email: hatazawa@tracer.med.osaka-u.ac.jp (JH); yuji@neurol.med.osaka-u.ac.jp (YN)

☯ These authors contributed equally to this work.

Introduction

Multiple sclerosis (MS) is an inflammatory demyelinating autoimmune disease of the CNS [1]. Although MRI is recognized as the most informative surrogate marker [2], the diagnostic value of MRI in MS remains insufficient [3]. Glial activation is a key feature in the neuroinflammatory MS pathology, and glial activation from the early phase of MS is suggested by a MRS study [4]. Microglial activation has also been shown in PET studies [5,6]. However, astrocyte activation in MS has not been evaluated in vivo due to the lack of an appropriate radioligand, despite the astrocytosis observed from the early phase of disease and the important role potentially played by astrocytes [4,7,8].

Acetate is converted into fatty acids by the key enzyme acetyl-CoA synthase and metabolized in the citric acid cycle. ^{11}C-acetate has been used as a tracer to evaluate cardiac oxidative metabolism [9] and later used as a PET biomarker in patients with renal cell carcinoma, hepatocellular carcinoma, prostate cancer, and multiple myeloma [10,11,12,13]. In the CNS, ^{11}C-acetate PET has proven useful for the diagnosis of astrocytoma [14] because acetate is preferentially absorbed into astrocytes by the monocarboxylate transporter (MCT) [15,16]. Notably, the expression of MCT is increased in MS brains [17]. Therefore, we surmised that ^{11}C-acetate PET could be a useful diagnostic tool in combination with MRI, and we investigated the utility of ^{11}C-acetate PET for the diagnosis of MS and evaluated the astrocyte activity in the MS brain.

Materials and Methods

Subjects and clinical evaluation

Six patients with relapsing-remitting MS were evaluated. All patients were in the remission phase. Disability was assessed based

Table 1. Patient data and demographics.

	sex	age	type	therapy	EDSS score	Disease duration (y)	GM SUVt	WM SUVt	WM/GM ratio
MS 1	F	47	RR	IFNβ, MTX	7	10.3	1.0494	0.9415	0.8972
MS 2	F	45	RR	IFNβ	2	6.8	1.1069	1.0529	0.9512
MS 3	F	48	RR	IFNβ	1	5.7	1.0282	0.8874	0.8631
MS 4	F	53	RR	IFNβ	2.5	7.4	1.0837	0.9434	0.8705
MS 5	F	34	RR	-	4	3.3	0.9633	0.8244	0.8558
MS 6	F	49	RR	-	1	1.4	1.0336	0.9044	0.8750
HV 1	F	54					0.9149	0.7320	0.8001
HV 2	F	61					0.9671	0.8121	0.8397
HV 3	F	41					0.9518	0.7789	0.8183
HV 4	F	67					0.9341	0.7946	0.8507
HV 5	F	62					0.9449	0.8021	0.8489
HV 6	F	63					0.9758	0.8096	0.8297

MS = multiple sclerosis, HV = healthy volunteer, RR = relapsing-remitting multiple sclerosis, IFNβ = interferon beta treatment, MTX = Mitoxantrone, EDSS = Expanded Disability Status Scale, SUV = standardized uptake value.

doi:10.1371/journal.pone.0111598.t001

on the Expanded Disability Status Scale (EDSS) [18]. Six healthy volunteers (HV) served as normal controls (Table 1). This study was approved by the Ethics Committee of Osaka University Hospital, and written informed consent was obtained from each participant.

MRI

MRI was performed using a GE SIGNA HDxt 3.0-T or a Phillips Achieva 3.0-T scanner. Three-dimensional (3D) structural MRI was performed for each subject using a T1-weighted spoiled gradient recalled (SPGR) sequence (axial plane; slice thickness, 0.90/0.95 mm; matrix size, 512×512; in-plane resolution, 0.47×0.47 mm; TR, 2.144 to 2.192/2.477 to 2.53 ms; TE, 6.908 to 7.108/6.000; flip angle, 18°/15°) and T2-weighted two-dimensional fast spin echo sequences (axial plane; FOV 250 mm; matrix size, 512×512; slice thickness, 5 mm; interslice gap, 1 to 1.5 mm; TE, 89/80 ms; TR, 4500/3000 ms).

PET

PET was performed using a SET-3000 GCT/X scanner (Shimadzu Corp., Kyoto, Japan). ^{11}C-acetate was synthesized by carbonation of Grignard reagent followed by acid hydrolysis. ^{11}C-carbon dioxide reacted with methylmagnesium bromide followed by hydrolysis with hydrochloric acid to yield ^{11}C acetic acid [19]. The radio chemical purity was greater than 98%. A total of 370 MBq of the tracer was administered intravenously, and a 20-min emission acquisition was initiated 20 min later. PET images were obtained in a 3-D mode. The images were reconstructed using a filtered-back projection method after 3D Gaussian smoothing with a 6-mm full width at half maximum (FWHM). Scatter correction was performed using a hybrid dual-energy window method combined with a convolution-subtraction method, and the true scatter-free component of the standard photopeak window was estimated sonographically. All PET images were reconstructed in 256×256×99 anisotropic voxels, with each voxel measuring 1×1×2.6 mm.

Data analysis

Whole brain VOI analysis. All procedures were performed using a personal computer (DELL Precision T7400; DELL Inc., Round Rock, TX, USA) running on Microsoft Windows 7 (Microsoft Corp., Redmond, WA, USA). The 3D T1-weighted MRI scan was re-sliced in the native space of each subject using a 1.0×1.0×1.0 mm voxel size. The results were first categorized as GM, WM, and CSF, then spatially normalized using the unified model [20] of Statistical Parametric Mapping (SPM) 8 (Wellcome Department of Imaging Neuroscience: http://www.fil.ion.ucl.ac.uk/spm/) according to the optimized voxel-based morphometry (VBM) protocol [21]. This generated both spatial normalization matrices and inverse spatial normalization matrices. The resulting normalized GM map was transformed into native space using an inverse spatial normalization matrix. To generate VOI for GM and/or WM, binary mask images for the GM and/or WM were created using the segmented images in the native space of each subject. The binary mask image boundary was set at 35% of the maximum GM or WM concentration as described in previous studies [22,23].

The ^{11}C-acetate PET images were co-registered with the resliced 3D T1-weighted MRI using the SPM8 registration function based on the mutual information. The co-registration precision was inspected with the "Check Registration" tool in SPM8. Then, the co-registered PET images were spatially transformed using normalization and/or inverse normalization matrices identical to those generated in the previously described

automatic segmentation process. The ^{11}C -acetate uptake in the GM and WM VOI was analyzed using the binary masks within the native space.

To minimize contamination from the spill-in effect of adjacent brain segments, the spill-in-free VOIs of GM and WM were generated by the VOI erosion process. First, the binary masks were blurred by convolution using the point spread function of the PET scanner (presumably a simple isotropic Gaussian kernel with a FWHM of 8 mm). The spill-in-free gray matter mask $\hat{G}$ is expressed as follows:

$$\hat{G} = \{x \in G | \tilde{W}(x) < 0.1\},$$

where x is a voxel, G is the gray matter binary mask, and $\tilde{W}(x)$ is the blurred image of the white matter binary mask (i.e. spill-in fraction from the white matter to the voxel x). The spill-in-free white matter mask was also constructed as described above. Spill-in from CSF was assumed as zero. VOI analysis for ^{11}C-acetate uptake using spill-in-free GM and WM masks was also performed (Figure S1).

The relative standardized uptake value (SUVt) served as the uptake indicator for analysis; the regional standardized uptake value (SUV) was divided by the mean SUV within the bilateral thalami of each subject. The Mann–Whitney U test was performed to determine significance of ^{11}C -acetate SUVt differences between MS and HV. The significance level was designated at $p<0.05$.

Voxel-based statistical analysis. Voxel-based whole brain SUVt in the MS and HV groups was compared using Statistical Parametric Mapping (SPM) 8 (Wellcome Department of Imaging Neuroscience). The spatially normalized PET images were smoothed using a 12-mm FWHM isotropic Gaussian kernel, which conditions the residuals to conform more closely to the Gaussian random field model underlying the statistical adjustment of the p values. The SPM statistical model used voxel-by-voxel "two-sample T-test with covariates," which designated age as a nuisance variable in order to detect voxels showing a significant age-adjusted SUVt difference between the MS and HV groups.

11C-acetate uptake and the MR images correlation assessment. The T2 and T1 black hole lesions were independently recorded visually by three observers. T1 black holes were defined as visible hypointense regions on the T1- weighted images coincident with a high signal intense region on the T2-weighted images. Each MRI mask image was divided into its hemispheres to create the hemispheric VOIs. Pearson product moment correlation analyses were performed to assess the association between the number of MRI lesions, and the SUV of ^{11}C-acetate was accessed from the hemispheric VOIs of the GM and WM. Statistical significance was designated at $p<0.05$.

Statistical analysis

The data in Fig 1 and Table S1 were analyzed using the Mann–Whitney U test. ANCOVA was used to assess the differences between age-adjusted groups illustrated in Fig 2B–G, and Pearson product moment correlation analyses were performed for data in Fig 3, SPSS 14.J was used for statistical analysis.

Results

VOI analysis of the ^{11}C-acetate SUV revealed that the mean SUV was higher in the MS patients than in the HV in all regions assessed (Fig 1A). To evaluate the regional distribution of ^{11}C-acetate uptake independent of physiologic variation in the whole brain, we calculated the relative uptake value (SUVt), which is the regional SUV divided by the mean SUV within the bilateral thalami of each participant (Fig 1B). The thalamus served as the reference region because it is rarely involved in MS pathology [24], and the SUV difference between the thalamus of HV and MS patients was the least among brain regions, as shown in Fig 1A. Each regional SUVt in the MS patients were increased particularly in the parietal, occipital, and insula regions.

Spatially normalized group mean images of ^{11}C-acetate SUVt automatically segmented based on MRI showed increased uptake in both WM and GM in MS patients (Fig 2A). The SUVt of MS patients was significantly higher than that of HV in both WM ($p = 0.002$) and GM ($p = 0.001$). In addition, all six MS patients had a significantly higher WM/GM SUV ratio than the six HV ($p = 0.009$) (Fig 2B–D). This trend was consistently observed even after accommodating spill-in effect from adjacent brain segments (Fig 2E–G). Collectively, the ^{11}C-acetate uptake significantly increased in both the WM and GM of MS patients, and this increase was more predominant in WM. The whole brain SPM analysis revealed a significant increase in SUVt of voxel cluster in MS patients compared to HV, primarily in the subcortical frontal, parietal, and occipital regions; no voxels showed a significantly lower SUVt in MS patients compared to HV (Fig 2H).

The voxel-based t-statistic for the WM tracts showed a significantly increased mean T-score, predominantly in the superior longitudinal fasciculus, posterior thalamic radiation, and sagittal stratum, with the highest local maximum T-score in the corpus callosum (Table S2).

We then assessed potential correlation between ^{11}C-acetate SUV and MRI brain lesions. The mean SUV in WM was significantly correlated to the number of T1 black holes ($R^2 = 0.5059$, $p = 0.009$) and T2 lesions ($R^2 = 0.4594$, $p = 0.015$) (Fig 3A, B). The mean SUV in GM also correlated to the number of T1 black holes ($R^2 = 0.4088$, $p = 0.025$) and T2 lesions ($R^2 = 0.3952$, $p = 0.029$) (Fig 3C, D). The correlation to the EDSS score and disease duration did not reach statistical significance.

Discussion

There have been few studies imaging astrocytes in vivo using ^{11}C-acetate PET. In MS, astrocyte proliferation [25] and formation of scars composing a dense network of hypertrophic cells are characteristics of the MS histopathology [8]. An increased MCT expression in astrocytes within MS lesions was recently shown by immunohistochemical analysis [17], which suggest an increase in astrocyte metabolism. However, latent autoantibody-mediated astrocyte damage [26] supposedly decreases the metabolic activity, and therefore, the metabolic activity of astrocytes in MS brains remains undetermined. In this study, we observed a significantly increased brain uptake of the radioligand ^{11}C-acetate in MS patients. Our study revealed for the first time that astrocytes are generally activated in MS brains based on the acetate metabolism.

Representative studies showed that a higher value in the kinetic parameter, which indicates the washout level of ^{11}C-acetate, reflects the astrocyte reactivity in normal rats and healthy humans [27]. In MS, however, compared to HV, the pathologic changes in the severity of ^{11}C-acetate accumulation may be much more prominent than the changes related to physiologic activation in healthy humans. Therefore, a slight increase in the washout speed may be inapparent in the PET SUV in MS. Furthermore, because the perfusion in the normal appearing white matter decreased in MS [28], the increase in ^{11}C-acetate uptake by static PET may be underestimated due to a reduced CBF in MS.

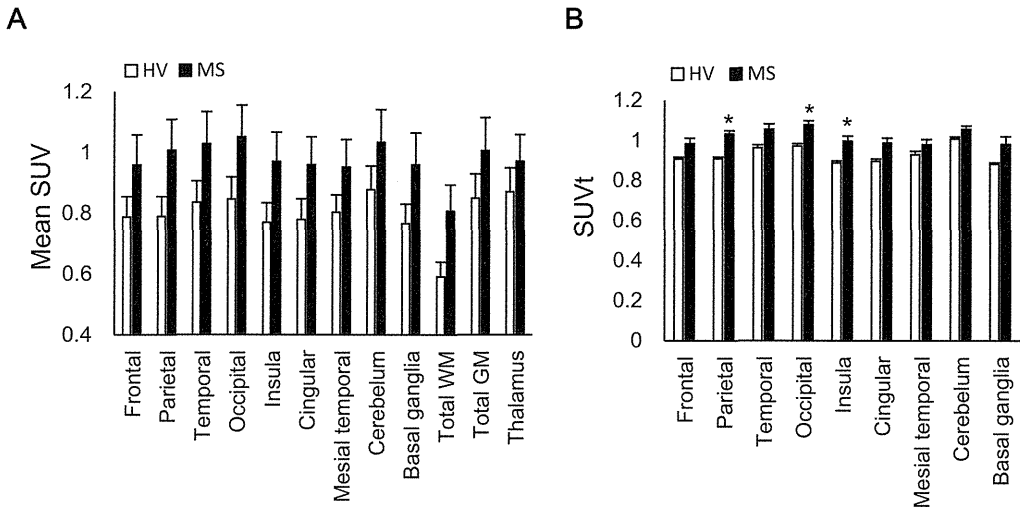

Figure 1. ^{11}C-acetate CNS biodistribution. (A)Mean standardized uptake value (SUV) of each lesion. (B) Relative SUV compared to that of the thalamus (SUVt). Data are expressed as the mean ± standard error of the mean (SEM) (n = 6). The Mann–Whitney *U* test showed a significant difference in the median between the HV and MS groups (*:p<0.0055 after Bonferroni correction). HV = healthy volunteers, MS = multiple sclerosis.
doi:10.1371/journal.pone.0111598.g001

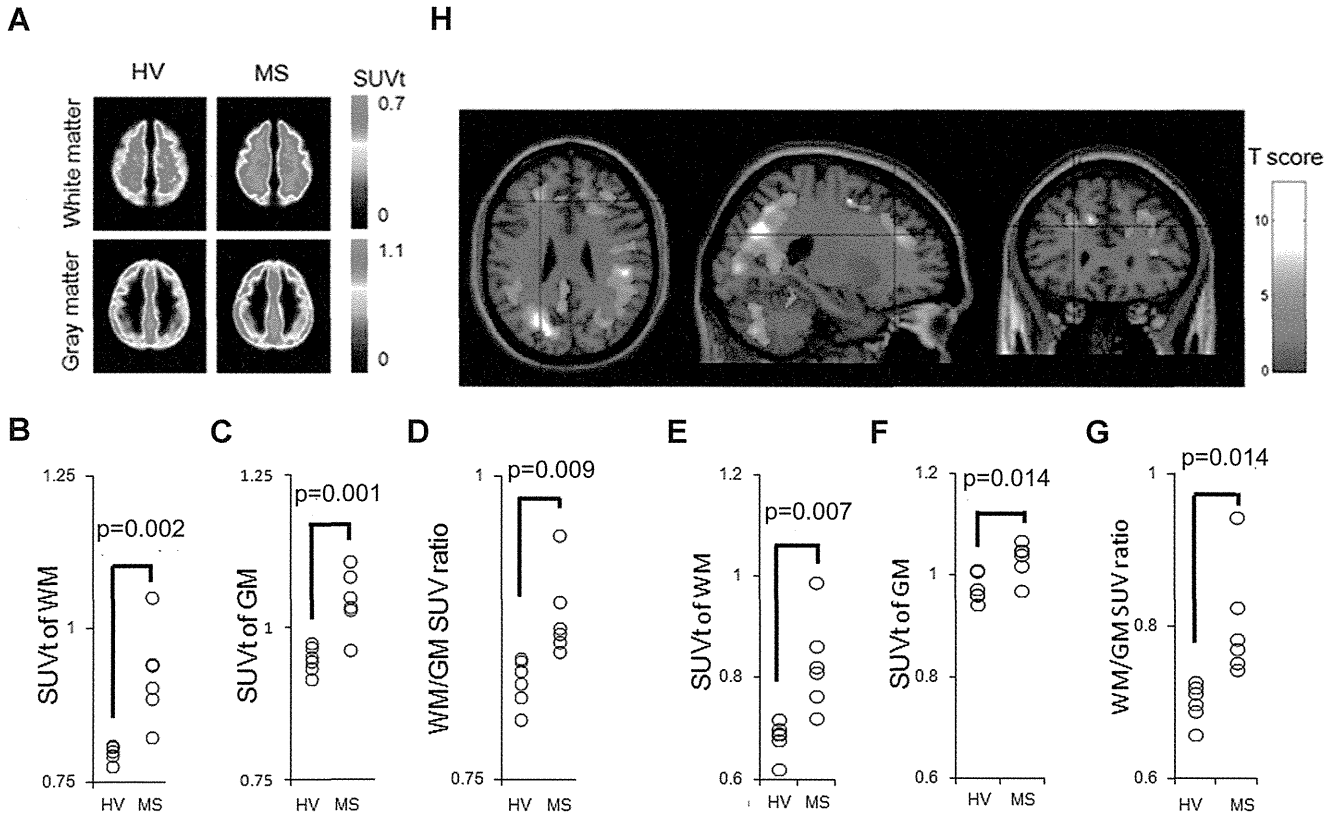

Figure 2. ^{11}C-acetate uptake distribution and quantification in MS patients. (A)Spatially normalized group mean images of ^{11}C-acetate SUVt automatically segmented based on MRI. VOI analysis summarizing the mean SUVt in WM (B) and GM (C), and the WM/GM SUV ratio (D) in the HV and MS groups. The identical analysis performed using spill-in-free VOIs are also shown (E–G). The p-value was calculated using the analysis of covariance to adjust the variance of age. (H) The SPM analysis result is overlaid onto the T1-weighted brain MRI template. Colored voxels indicate T-scores representing significantly increased ^{11}C-acetate uptake (SUVt) in patients with MS compared to HV patients. The spatially normalized PET images were smoothed for the analysis using a 12-mm FWHM isotropic Gaussian kernel. The significance thresholds are corrected for multiple comparisons at the cluster level with a p-value of 0.05 (family-wise error correction). SUV: standardized uptake value.
doi:10.1371/journal.pone.0111598.g002

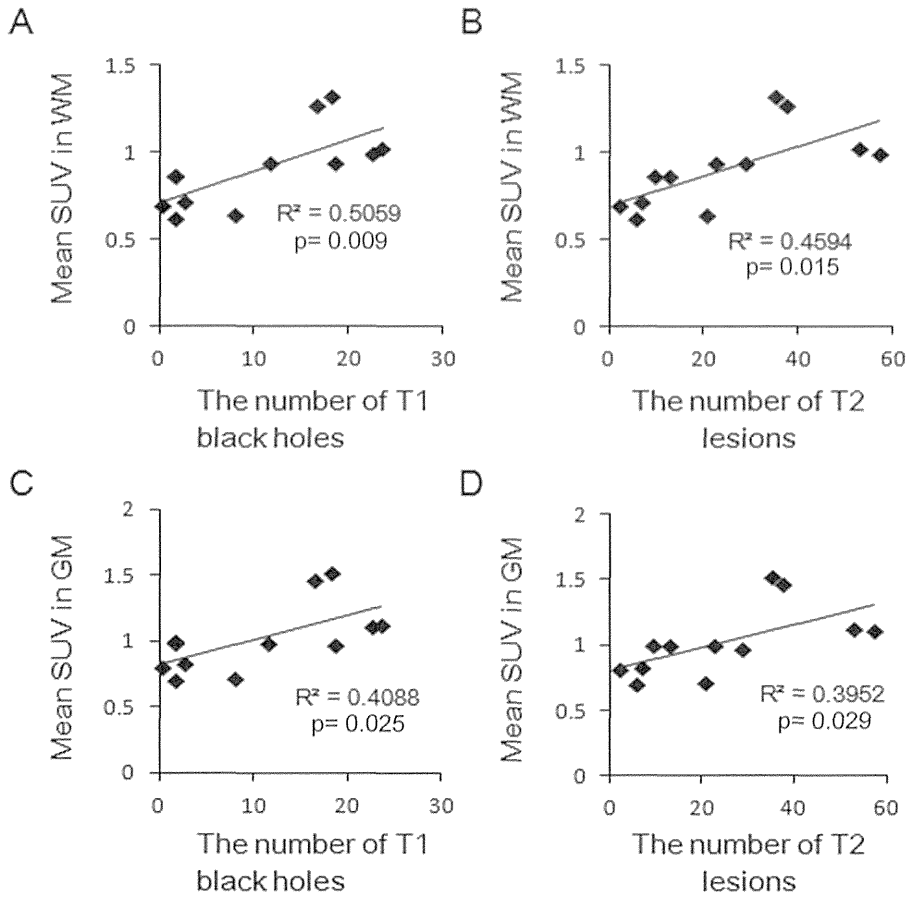

Figure 3. Correlation between ^{11}C-acetate SUV and the number of MRI lesions in patients with MS. Correlation between ^{11}C-acetate SUV in WM or GM and the number of T1 black holes (A, C) or T2 lesions (B, D) in each hemisphere of the six MS patients. SUV: standardized uptake value.
doi:10.1371/journal.pone.0111598.g003

The increased uptake was more pronounced in the WM, although a significant increase was observed in both the WM and GM. A significantly increased uptake was observed primarily within the subcortical WM on the voxel-based statistical analysis (Fig. 2H). On the voxel-based statistical analysis of the WM tracts, the distribution of the increased acetate uptake was similar to that in regions of axonal damage in DTI studies (Table S2). Recent voxel- and tract-based analyses in DTI studies revealed widespread damage to the subcortical WM, particularly in the sagittal stratum, corpus callosum, posterior thalamic radiation, and corona radiata [29]. These data suggested that the region-dependent increased acetate uptake was induced by the reactive astrocyte coexisting with heterogeneously dispersed MS lesions detected in DTI studies (Fig. 2H and Table S2). Although inflammatory WM demyelination detected by conventional MRI is a cardinal feature of MS, pathologic changes exist even in normal appearing WM and GM [30]. Astrocyte pathology precedes demyelination in an animal model [31]; astrocyte hypertrophy occurs at the leading edge of acute MS lesions, followed later by astrocytic scarring [8]. Thus, the altered astrocyte activation is presumably involved in MS pathophysiology [4,7,32]. Correlation between the radial diffusivity quantified by DTI and T1 black hole formation are recognized markers of axonal loss and tissue destruction [33,34]. In the present study, the strongest correlation was detected between the mean SUV in WM and the T1 black hole number, suggesting that the mean SUV may correlate with axonal damage. The mean SUV in GM also increased and correlated with the number of MRI lesions, suggesting cortical astrocyte involvement in MS pathology. Cortical involvement and subsequent cognitive decline occur in approximately half of MS patients [35]. However, little information exists on the pathophysiologic involvement of cortical astrocytes [36]. Normally, astrocytes supply lactate to neurons for oxidation [37], and metabolic dysfunction of neurons and glial cell activation likely occurs in the MS brain [25]. Moreover, astrocytes are associated with preclinical axonal damage in an animal model of MS [38]. These results suggest that the increased ^{11}C-acetate uptake within GM may reflect astrocyte-associated cortical damage in MS.

The present study has a few limitations. First, ^{11}C-acetate uptake in MS plaques was not assessed separately because most plaques were so small that a partial volume effect caused by the relatively low resolution of PET was inevitable. Second, the analysis was performed on static PET data instead of kinetic parameters. In the present study, the data acquired between 20 to 40 min after tracer administration were summed to build static uptake images because the time activity curve stabilized after 20 min (data not shown). Regional uptake distribution may be contaminated by the dispersion of radioactive metabolites. However, in our study, 1-^{11}C-acetate was used, and its dispersion of labeled metabolites was the smallest among the various types of acetate tracers [39,40]. In addition, because almost all the tracer was first absorbed through MCT-1 expressed within astrocytes according to their reactivity, the summed radioactivity is thought to reflect the first uptake of ^{11}C- acetate and its subsequent

metabolism by reactive astrocytes. Finally, because the mean age was higher in the control group than in the MS group, we used the ANCOVA to assess the differences among the age-adjusted SUVt. Although the mean age of MS patients was generally lower than that of the healthy volunteers, age did not significantly affect the increased uptake of ^{11}C-acetate in MS patients.

Conclusions

The present study suggests that the pathologic white matter changes in patients with MS can be detected by non-invasive static ^{11}C-acetate PET, which may be an effective MS diagnostic tool. Development of clinically applicable monocarbonic acid tracers labeled with longer half-life radioactive nuclides are needed, as are further studies enrolling more participants, including those in the early and relapse phases.

Supporting Information

Figure S1 Binary mask imaging parameters for VOI analysis. The scheme of VOI analysis is described. A: ^{11}C-acetate PET, B: 3D MRI, C: Co-registration, D: Spatial normalization to the MNI space, E/F: Segmented GM/WM map in the MNI space, G/H: GM/WM binarized mask in the original space of the subject, I/J: Eroded version of G/H for spill-in-free VOI analysis, K–N: GM/WM masks overlaid onto PET in the original space of the subject. MNI: montreal neurological institute. f: Transformation matrix for spatial normalization, f^{-1}: Inverse of the transformation.
(TIF)

Table S1 Relative ^{11}C-acetate biodistribution in the CNS. The mean SUVt of each lesion in the CNS was analyzed and for group comparison between HV and MS patients, the Mann–Whitney *U* test was performed.
(DOC)

Table S2 Regional T-scores from voxel-based statistical comparison in WM. Voxel-based statistical comparison in white matter tracts was performed. The positive T-scores indicate an increased ^{11}C-acetate uptake in the MS patients compared to the HV.
(DOC)

Text S1 Supplementary methods. Methods for "Voxel-based statistical analysis for WM tracts" are described with references.
(DOC)

Acknowledgments

We thank Dr. Hisashi Tanaka, Dr. Yoshiyuki Watanabe, Dr. Kayako Isohashi, Mr. Koichi Fujino, Mr. Yasukazu Kanai, Mr. Sadahiro Naka, and the staff of the Department of Nuclear Medicine and the Cyclotron staff of Osaka University Hospital for their technical support in performing the studies.

Author Contributions

Conceived and designed the experiments: YN HM JH. Performed the experiments: HK ES. Analyzed the data: KT HK TO TK TS. Wrote the paper: KT HK YN.

References

1. Compston A, Coles A (2002) Multiple sclerosis. Lancet 359: 1221–1231.
2. Sormani MP, Bruzzi P (2013) MRI lesions as a surrogate for relapses in multiple sclerosis: a meta-analysis of randomised trials. Lancet Neurol 12: 669–676.
3. Odenthal A, Coulthard C (2014) The Prognostic Utility of MRI in Clinically Isolated Syndrome: A Literature Review. AJNR Am J Neuroradiol.
4. Fernando KT, McLean MA, Chard DT, MacManus DG, Dalton CM, et al. (2004) Elevated white matter myo-inositol in clinically isolated syndromes suggestive of multiple sclerosis. Brain 127: 1361–1369.
5. Banati RB, Newcombe J, Gunn RN, Cagnin A, Turkheimer F, et al. (2000) The peripheral benzodiazepine binding site in the brain in multiple sclerosis: quantitative in vivo imaging of microglia as a measure of disease activity. Brain 123 (Pt 11): 2321–2337.
6. Politis M, Giannetti P, Su P, Turkheimer F, Keihaninejad S, et al. (2012) Increased PK11195 PET binding in the cortex of patients with MS correlates with disability. Neurology 79: 523–530.
7. Black JA, Newcombe J, Waxman SG (2010) Astrocytes within multiple sclerosis lesions upregulate sodium channel Nav1.5. Brain 133: 835–846.
8. Brosnan CF, Raine CS (2013) The astrocyte in multiple sclerosis revisited. Glia 61: 453–465.
9. Brown M, Marshall DR, Sobel BE, Bergmann SR (1987) Delineation of myocardial oxygen utilization with carbon-11-labeled acetate. Circulation 76: 687–696.
10. Oyama N, Okazawa H, Kusukawa N, Kaneda T, Miwa Y, et al. (2009) 11C-Acetate PET imaging for renal cell carcinoma. Eur J Nucl Med Mol Imaging 36: 422–427.
11. Ho CL, Yu SC, Yeung DW (2003) 11C-acetate PET imaging in hepatocellular carcinoma and other liver masses. J Nucl Med 44: 213–221.
12. Oyama N, Akino H, Kanamaru H, Suzuki Y, Muramoto S, et al. (2002) 11C-acetate PET imaging of prostate cancer. J Nucl Med 43: 181–186.
13. Lin C, Ho CL, Ng SH, Wang PN, Huang Y, et al. (2014) (11)C-acetate as a new biomarker for PET/CT in patients with multiple myeloma: initial staging and postinduction response assessment. Eur J Nucl Med Mol Imaging 41: 41–49.
14. Liu RS, Chang CP, Chu LS, Chu YK, Hsieh HJ, et al. (2006) PET imaging of brain astrocytoma with 1-11C-acetate. Eur J Nucl Med Mol Imaging 33: 420–427.
15. Waniewski RA, Martin DL (1998) Preferential utilization of acetate by astrocytes is attributable to transport. J Neurosci 18: 5225–5233.
16. Hosoi R, Okada M, Hatazawa J, Gee A, Inoue O (2004) Effect of astrocytic energy metabolism depressant on 14C-acetate uptake in intact rat brain. J Cereb Blood Flow Metab 24: 188–190.
17. Nijland PG, Michailidou I, Witte ME, Mizee MR, van der Pol SM, et al. (2014) Cellular distribution of glucose and monocarboxylate transporters in human brain white matter and multiple sclerosis lesions. Glia 62: 1125–1141.
18. Kurtzke JF (1983) Rating neurologic impairment in multiple sclerosis: an expanded disability status scale (EDSS). Neurology 33: 1444–1452.
19. Ishiwata K, Ishii S-I, Senda M (1995) Successive preparation of 11C labeled sodium acetate and/or sodium hexanoate. Applied Radiation and Isotopes 46: 1035–1037.
20. Ashburner J, Friston KJ (2005) Unified segmentation. Neuroimage 26: 839–851.
21. Good CD, Johnsrude IS, Ashburner J, Henson RN, Friston KJ, et al. (2001) A voxel-based morphometric study of ageing in 465 normal adult human brains. Neuroimage 14: 21–36.
22. Hosoi R, Matsuyama Y, Hirose S, Koyama Y, Matsuda T, et al. (2009) Characterization of (14)C-acetate uptake in cultured rat astrocytes. Brain Res 1253: 69–73.
23. Kato H, Shimosegawa E, Isohashi K, Kimura N, Kazui H, et al. (2012) Distribution of cortical benzodiazepine receptor binding in right-handed healthy humans: a voxel-based statistical analysis of iodine 123 iomazenil SPECT with partial volume correction. AJNR Am J Neuroradiol 33: 1458–1463.
24. Brownell B, Hughes JT (1962) The distribution of plaques in the cerebrum in multiple sclerosis. J Neurol Neurosurg Psychiatry 25: 315–320.
25. Chard DT, Griffin CM, McLean MA, Kapeller P, Kapoor R, et al. (2002) Brain metabolite changes in cortical grey and normal-appearing white matter in clinically early relapsing-remitting multiple sclerosis. Brain 125: 2342–2352.
26. Srivastava R, Aslam M, Kalluri SR, Schirmer L, Buck D, et al. (2012) Potassium channel KIR4.1 as an immune target in multiple sclerosis. N Engl J Med 367: 115–123.
27. Wyss MT, Weber B, Treyer V, Heer S, Pellerin L, et al. (2009) Stimulation-induced increases of astrocytic oxidative metabolism in rats and humans investigated with 1-11C-acetate. J Cereb Blood Flow Metab 29: 44–56.
28. De Keyser J, Steen C, Mostert JP, Koch MW (2008) Hypoperfusion of the cerebral white matter in multiple sclerosis: possible mechanisms and pathophysiological significance. J Cereb Blood Flow Metab 28: 1645–1651.
29. Dineen RA, Vilisaar J, Hlinka J, Bradshaw CM, Morgan PS, et al. (2009) Disconnection as a mechanism for cognitive dysfunction in multiple sclerosis. Brain 132: 239–249.
30. Bjartmar C, Kinkel RP, Kidd G, Rudick RA, Trapp BD (2001) Axonal loss in normal-appearing white matter in a patient with acute MS. Neurology 57: 1248–1252.
31. Sharma R, Fischer MT, Bauer J, Felts PA, Smith KJ, et al. (2010) Inflammation induced by innate immunity in the central nervous system leads to primary

astrocyte dysfunction followed by demyelination. Acta Neuropathol 120: 223–236.
32. Choi JW, Gardell SE, Herr DR, Rivera R, Lee CW, et al. (2011) FTY720 (fingolimod) efficacy in an animal model of multiple sclerosis requires astrocyte sphingosine 1-phosphate receptor 1 (S1P1) modulation. Proc Natl Acad Sci U S A 108: 751–756.
33. Naismith RT, Xu J, Tutlam NT, Scully PT, Trinkaus K, et al. (2010) Increased diffusivity in acute multiple sclerosis lesions predicts risk of black hole. Neurology 74: 1694–1701.
34. Sahraian MA, Radue EW, Haller S, Kappos L (2010) Black holes in multiple sclerosis: definition, evolution, and clinical correlations. Acta Neurol Scand 122: 1–8.
35. Blinkenberg M, Rune K, Jensen CV, Ravnborg M, Kyllingsbaek S, et al. (2000) Cortical cerebral metabolism correlates with MRI lesion load and cognitive dysfunction in MS. Neurology 54: 558–564.
36. Vercellino M, Merola A, Piacentino C, Votta B, Capello E, et al. (2007) Altered glutamate reuptake in relapsing-remitting and secondary progressive multiple sclerosis cortex: correlation with microglia infiltration, demyelination, and neuronal and synaptic damage. J Neuropathol Exp Neurol 66: 732–739.
37. Hyder F, Patel AB, Gjedde A, Rothman DL, Behar KL, et al. (2006) Neuronal-glial glucose oxidation and glutamatergic-GABAergic function. J Cereb Blood Flow Metab 26: 865–877.
38. Wang D, Ayers MM, Catmull DV, Hazelwood LJ, Bernard CC, et al. (2005) Astrocyte-associated axonal damage in pre-onset stages of experimental autoimmune encephalomyelitis. Glia 51: 235–240.
39. Van den Berg CJ, Mela P, Waelsch H (1966) On the contribution of the tricarboxylic acid cycle to the synthesis of glutamate, glutamine and aspartate in brain. Biochem Biophys Res Commun 23: 479–484.
40. Wyss MT, Magistretti PJ, Buck A, Weber B (2011) Labeled acetate as a marker of astrocytic metabolism. J Cereb Blood Flow Metab 31: 1668–1674.

PLOS ONE

Genetic and Infectious Profiles Influence Cerebrospinal Fluid IgG Abnormality in Japanese Multiple Sclerosis Patients

Satoshi Yoshimura[1], Noriko Isobe[1], Takuya Matsushita[1], Katsuhisa Masaki[1], Shinya Sato[1], Yuji Kawano[1], Hirofumi Ochi[2], Jun-ichi Kira[1]*

1 Department of Neurology, Neurological Institute, Graduate School of Medical Sciences, Kyushu University, Fukuoka, Japan, **2** Department of Molecular and Genetic Medicine, Ehime University Graduate School of Medicine, Ehime, Japan

Abstract

Background: Abnormal intrathecal synthesis of IgG, reflected by cerebrospinal fluid (CSF) oligoclonal IgG bands (OBs) and increased IgG index, is much less frequently observed in Japanese multiple sclerosis (MS) cohorts compared with Western cohorts. We aimed to clarify whether genetic and common infectious backgrounds influence CSF IgG abnormality in Japanese MS patients.

Methodology: We analyzed *HLA-DRB1* alleles, and IgG antibodies against *Chlamydia pneumoniae*, *Helicobacter pylori*, Epstein-Barr virus nuclear antigen (EBNA), and varicella zoster virus (VZV) in 94 patients with MS and 367 unrelated healthy controls (HCs). We defined CSF IgG abnormality as the presence of CSF OBs and/or increased IgG index (>0.658).

Principal Findings: CSF IgG abnormality was found in 59 of 94 (62.8%) MS patients. CSF IgG abnormality-positive patients had a significantly higher frequency of brain MRI lesions meeting the Barkhof criteria compared with abnormality-negative patients. Compared with HCs, CSF IgG abnormality-positive MS patients showed a significantly higher frequency of *DRB1*1501*, whereas CSF IgG abnormality-negative patients had a significantly higher frequency of *DRB1*0405*. CSF IgG abnormality-positive MS patients had a significantly higher frequency of anti-*C. pneumoniae* IgG antibodies compared with CSF IgG abnormality-negative MS patients, although there was no difference in the frequency of anti-*C. pneumoniae* IgG antibodies between HCs and total MS patients. Compared with HCs, anti-*H. pylori* IgG antibodies were detected significantly less frequently in the total MS patients, especially in CSF IgG abnormality-negative MS patients. The frequencies of antibodies against EBNA and VZV did not differ significantly among the groups.

Conclusions: CSF IgG abnormality is associated with Western MS-like brain MRI features. *DRB1*1501* and *C. pneumoniae* infection confer CSF IgG abnormality, while *DRB1*0405* and *H. pylori* infection are positively and negatively associated with CSF IgG abnormality-negative MS, respectively, suggesting that genetic and environmental factors differentially contribute to MS susceptibility according to the CSF IgG abnormality status.

Citation: Yoshimura S, Isobe N, Matsushita T, Masaki K, Sato S, et al. (2014) Genetic and Infectious Profiles Influence Cerebrospinal Fluid IgG Abnormality in Japanese Multiple Sclerosis Patients. PLoS ONE 9(4): e95367. doi:10.1371/journal.pone.0095367

Editor: Akio Suzumura, Research Inst. of Environmental Med., Nagoya Univ., Japan

Received December 10, 2013; **Accepted** March 26, 2014; **Published** April 15, 2014

Funding: This work was supported in part by a Health and Labour Sciences Research Grant on Intractable Diseases (H20-Nanchi-Ippan-016) from the Ministry of Health, Labour and Welfare, Japan, and a Grant-in-Aid (B; No. 22390178) from the Ministry of Education, Culture, Sports, Science and Technology, Japan. The funders had no role in study design, data collection and analysis, decision to publish, or preparation of the manuscript.

Competing Interests: Jun-ichi Kira is an advisory board member for Merck Serono and a consultant for Biogen Idec Japan. He has received payment for lectures from Bayer Schering Pharma, Cosmic Cooperation, and Biogen Idec Japan. Takuya Matsushita received a grant and payment for manuscript preparation and development of educational presentations from Bayer Schering Pharma, and also received a payment for the development of educational presentations from Mitsubishi Tanabe Pharma. This does not alter our adherence to PLOS ONE policies on sharing data and materials. Jun-ichi Kira is a PLOS ONE Editorial Board member. This does not alter our adherence to PLOS ONE Editorial policies and criteria.

* E-mail: kira@neuro.med.kyushu-u.ac.jp

Introduction

Multiple sclerosis (MS) is a chronic inflammatory demyelinating disease of the central nervous system (CNS) with a supposed autoimmune origin involving T and B cells [1]. Interplay between genetic and environmental factors is assumed to contribute to the pathogenesis of MS [2]. The largest genetic effect on MS susceptibility is conferred by the major histocompatibility complex class II genes. In Caucasians, the *HLA-DRB1*1501* allele is most strongly associated with MS, whereas the class I allele *HLA-A*0201* allele appears to be a protective allele [3]. In the Japanese population, we and others reported that conventional MS (CMS) is associated with *HLA-DRB1*1501*, while opticospinal MS (OSMS) is associated with *HLA-DPB1*0501* [4,5], but no associations were found with any HLA class I alleles [6]. Recently, we reported that *HLA-DRB1*0405* and *HLA-DPB1*0301* are susceptibility alleles, while *DRB1*0901* and *DPB1*0401* are protective alleles for Japanese MS when neuromyelitis optica (NMO) and NMO spectrum disorder (NMOSD) patients are excluded [7].

Among many potential environmental risk factors, infection is likely to play a significant role in the acquisition of MS susceptibility or resistance. One candidate infectious agent is Epstein-Barr virus (EBV), which is more prevalent in Caucasian MS patients than in healthy controls (HCs), and therefore considered to increase susceptibility to MS [8,9]. We recently found that the EBV infection rate has increased in a certain subgroup of Japanese MS patients not harboring *HLA-DRB1*0405*, a genetic risk factor for MS in the Japanese population, compared with HCs [7]. Since the first possible reported association between *Chlamydia pneumoniae* infection and MS [10], the significance of *C. pneumoniae* infection in MS has remained a matter of debate. We demonstrated that the anti-*C. pneumoniae* antibody positivity rate did not differ significantly between MS and HCs in Japanese [7], which is consistent with recent meta-analysis results [11]. We also found that the anti-*Helicobacter pylori* antibody positivity rate was lower among CMS patients than among HCs and OSMS patients in Japanese [12]. By contrast, the anti-*H. pylori* and anti-*C. pneumoniae* antibody positivity rates were increased in Japanese patients with NMO, especially in those with anti-aquaporin 4 (AQP4) antibodies [13,14].

Abnormal intrathecal synthesis of IgG, reflected by cerebrospinal fluid (CSF) oligoclonal IgG bands (OBs) and increased IgG index, is a significant diagnostic hallmark in MS. More than 90% of MS patients are positive for CSF OBs in Western countries [15,16]. However, this proportion appears to vary with ethnicity or geographical location, ranging from only 21–56% in Asian countries [17–21]. The presence of genetic influences on the OB phenotype is suggested by their associations in several populations. For example, the *HLA-DRB1*15* allele is associated with OB-positive MS [19,22,23] and the *HLA-DRB1*04* allele is associated with OB-negative MS [19,22]. Although the prognostic significance of OBs is conflicting, the absence of OBs predicted a relatively benign clinical course and lower disease severity in some early studies [24,25], but not all [18,26–29]. Focusing on MRI findings, some studies have postulated a potentially lower lesion load in OB-negative patients [25,29].

With this background, we aimed to investigate whether genetic and common infectious profiles influence CSF IgG abnormality in Japanese MS patients. In the present study, we focused on *HLA-DRB1* loci that are associated with MS in several populations, including Japanese. Among the infectious factors, we chose *C. pneumoniae*, *H. pylori*, EBV, and varicella zoster virus (VZV) infections, which could be potential environmental risk or protective factors for MS.

Methods

Participants

Ninety-four patients examined at the Department of Neurology, Kyushu University Hospital from 2006 to 2010 were enrolled. MS was defined using the 2005 revised McDonald criteria for MS [30]. NMO was defined as cases fulfilling the 2006 revised criteria for NMO [31]. We regarded patients as having an NMOSD when they fulfilled either two absolute criteria plus at least one supportive criterion, or one absolute criterion plus more than one supportive criterion from the 2006 NMO criteria, as previously described [7,14]. None of the MS patients met the above-mentioned NMO/NMOSD criteria. Patients with primary progressive MS were excluded from the study. Informed consent was obtained from the 94 patients as well as 367 unrelated HCs. Among the MS patients, 84 patients had RRMS and 10 had SPMS. The MS patients were clinically classified into two subtypes, conventional MS (CMS) and OSMS, as described previously [4]. There were 70 patients with CMS and 24 patients with OSMS. We collected demographic data from the patients by retrospective review of their medical records. These data included sex, age at onset, disease duration, Kurtzke's Expanded Disability Status Scale (EDSS) scores [32], annualized relapse rate, Progression Index [33], CSF OBs, IgG index, and brain MRI lesions meeting the Barkhof criteria for MS [34]. CSF IgG was tested in the acute phase in all cases. OBs were determined by isoelectric focusing, as the most sensitive method for OB determination [15,20]. OBs were considered positive when they were only detected in CSF and comprised at least two bands. The IgG index represents (CSF IgG/serum IgG)/(CSF albumin/serum albumin). The IgG index was considered to be increased if it was >0.658 [4]. Among the 92 MS patients assayed for CSF OBs, 42 were OB-positive and 50 were OB-negative. Among the 90 MS patients whose IgG index was assayed, 42 had elevation and 48 did not. In this study, we defined CSF IgG abnormality as the presence of CSF OBs and/or increased IgG index. This study was approved by the Kyushu University Hospital Ethics Committee. All individuals involved in this study signed a written informed consent.

MRI analysis

All MRI studies were performed using 1.5 T units (Magnetom Vision and Symphony; Siemens Medical Systems, Erlangen, Germany) as previously described [35]. Brain MRI lesions were evaluated according to the Barkhof criteria for MS [34].

HLA-DRB1 genotyping

The genotypes of the *HLA-DRB1* alleles from the subjects were determined by hybridization between the products of polymerase chain reaction amplification of the *HLA-DRB1* genes and sequence-specific oligonucleotide probes, as described previously [7].

Anti-AQP4 antibody assay

The presence of anti-AQP4 antibodies was assayed as described previously [36], using green fluorescent protein (GFP)-AQP4 (M1 isoform) fusion protein-transfected human embryonic kidney (HEK) cells. Serum samples diluted 1:4 were assayed for anti-AQP4 antibodies at least twice using identical samples, with the examiners blinded to the origin of the specimens. Samples that gave a positive result twice were deemed positive. When the judgment was equivocal, we measured the anti-AQP4 antibody levels using GFP-AQP4 (M23 isoform)-transfected HEK cells.

Detection of anti-*H. pylori*, anti-*C. pneumoniae*, anti-VZV, and anti-EBV nuclear antigen (EBNA) IgG antibodies

Serum anti-*C. pneumoniae*, anti-*H. pylori*, anti-EBNA, and anti-VZV IgG antibodies were measured using commercial ELISA kits (Vircell, Granada, Spain) in accordance with the manufacturer's instructions, as described previously [13]. Each antibody index was determined by dividing the optical density (OD) values for the target samples by the OD values for cut-off control samples and then multiplying by ten. As recommended by the manufacturer, an ELISA test index value was considered positive if higher than 11, equivocal if between 9 and 11, and negative if less than 9. According to the manufacturer's instructions, the ELISAs used in the present study have 100% sensitivity and 83% specificity for *H. pylori* infection and 100% sensitivity and 93% specificity for *C. pneumoniae* infection. Samples with equivocal results were retested

Table 1. Comparisons of the demographic features of MS patients according to the CSF IgG abnormality status.

	CSF IgG abnormality (+) (n = 59)	CSF IgG abnormality (−) (n = 35)	P value
Male:female	18:41	15:20	0.2669
Age at onset (years)[a]	30.54±12.12	34.06±15.70	0.4157
Disease duration (years)[a]	10.48±8.24	10.29±8.45	0.7899
EDSS score[a]	2.74±1.92	2.83±1.84	0.6420
Annualized relapse rate[a]	0.58±0.60	0.87±0.90	0.0946
Progression index[a]	0.39±0.39	0.90±2.00	0.4740
Barkhof criteria[b]	46/58 (79.3%)	16/34 (47.1%)	0.0025
OSMS with short spinal cord lesions[c]	13/59 (22.0%)	11/35 (31.4%)	0.3366

[a]Values represent the mean ± SD.
[b]Brain MRI lesions meeting the Barkhof criteria [34].
[c]Opticospinal form of MS with short spinal cord lesions extending less than three vertebral segments.
CSF, cerebrospinal fluid; EDSS, Kurtzke's Expanded Disability Status Scale; MS, multiple sclerosis.
doi:10.1371/journal.pone.0095367.t001

for confirmation, and if the samples were equivocal twice, they were considered negative.

Statistical analyses

The phenotype frequencies of the *HLA-DRB1* alleles were compared using the chi-square test, or Fisher's exact probability test when the criteria for the chi-square test were not fulfilled. Uncorrelated p-values (p^{uncorr}) were corrected by multiplying them by the number of comparisons, as indicated in the table footnotes (Bonferroni–Dunn's correction), to calculate the corrected p-values (p^{corr}). Fisher's exact probability test was used to compare sex, brain MRI lesions meeting the Barkhof criteria [34], and frequencies of antibodies against common infectious agents among the groups. Other demographic features were analyzed using the Wilcoxon rank sum test. We analyzed the trends in the proportions of patients among subgroups with advancing year of birth using the Cochran–Armitage trend test. All analyses were performed using JMP 8.0.3 (SAS Institute, Cary, NC). In all assays, values of $p<0.05$ were considered statistically significant.

Results

Relationships between CSF IgG abnormality status and demographic features in MS

Among the 94 MS patients, 59 (62.8%) were CSF IgG abnormality-positive and 35 were abnormality-negative. CSF IgG abnormality-positive patients had a significantly higher frequency of brain MRI lesions meeting the Barkhof criteria than abnormality-negative patients (46/58, 79.3% versus 16/34, 47.1%, $p = 0.0025$) (Table 1). The sex distribution, age at onset, disease duration, EDSS score, annualized relapse rate, Progression Index, and frequency of OSMS presentation with short spinal cord lesions (less than three vertebral segments) showed no associations with the presence or absence of CSF IgG abnormality (Table 1). The proportion of patients with CSF IgG abnormality did not change significantly with advancing year of birth ($p>0.1$) (Figure 1).

Correlation of CSF IgG abnormality according to clinical subtypes

The frequency of CSF IgG abnormality did not differ significantly between RRMS (52/84, 61.9%) and SPMS (7/10, 70%). Additionally, there was no significant difference in the frequency of CSF IgG abnormality between CMS (46/70, 65.7%) and OSMS (13/24, 54.2%).

HLA-DRB1 alleles in all MS patients

Compared with HCs, MS patients showed a significantly higher frequency of the *DRB1*0405* allele ($p^{corr} = 0.0196$, OR = 2.217, 95% CI = 1.389–3.539) and a significantly lower frequency of the *DRB1*0901* allele ($p^{corr} = 0.0084$, OR = 0.279, 95% CI = 0.135–0.575) (Table 2).

HLA-DRB1 alleles in MS patients according to the presence or absence of CSF IgG abnormality

Compared with HCs, CSF IgG abnormality-positive MS patients showed a significantly higher frequency of the *DRB1*1501* allele ($p^{corr} = 0.0392$, OR = 2.624, 95% CI = 1.432–4.809), whereas CSF IgG abnormality-negative MS

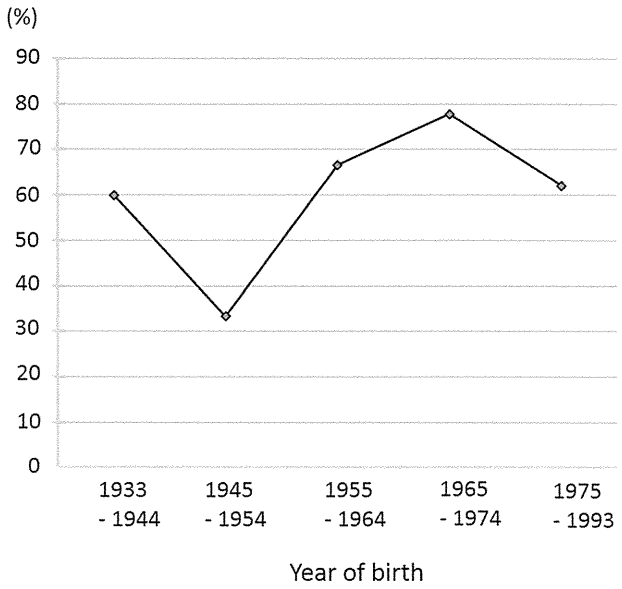

Figure 1. Proportions of patients with CSF IgG abnormality by year of birth. Among the MS patients, the proportion of patients with CSF IgG abnormality did not change significantly with advancing year of birth. CSF, cerebrospinal fluid; MS, multiple sclerosis.
doi:10.1371/journal.pone.0095367.g001

Table 2. Comparisons of the phenotype frequencies of the *HLA-DRB1* alleles.

DRB1*X	MS (n = 94)	CSF IgG abnormality (+) (n = 59)	CSF IgG abnormality (−) (n = 35)	HCs (n = 367)
0101 (%)	13 (13.8)	7 (11.9)	6 (17.1)	51 (13.9)
0301 (%)	0 (0.0)	0 (0.0)	0 (0.0)	2 (0.5)
0401 (%)	3 (3.2)	1 (1.7)	2 (5.7)	4 (1.1)
0403 (%)	4 (4.3)	4 (6.8)	0 (0.0)	18 (4.9)
0404 (%)	2 (2.1)	2 (3.4)	0 (0.0)	0 (0.0)
0405 (%)	42 (44.7)*[a]	22 (37.3)	20 (57.1)*[b]	98 (26.7)
0406 (%)	13 (13.8)	8 (13.6)	5 (14.3)	23 (6.3)
0407 (%)	0 (0.0)	0 (0.0)	0 (0.0)	2 (0.5)
0410 (%)	2 (2.1)	2 (3.4)	0 (0.0)	4 (1.1)
0701 (%)	0 (0.0)	0 (0.0)	0 (0.0)	2 (0.5)
0802 (%)	12 (12.8)	8 (13.6)	4 (11.4)	26 (7.1)
0803 (%)	11 (11.7)	9 (15.3)	2 (5.7)	58 (15.8)
0901 (%)	9 (9.5)*[c]	6 (10.2)	3 (8.6)	101 (27.5)
1001 (%)	0 (0.0)	0 (0.0)	0 (0.0)	4 (1.1)
1101 (%)	4 (4.3)	2 (3.4)	2 (5.7)	16 (4.4)
1106 (%)	0 (0.0)	0 (0.0)	0 (0.0)	1 (0.3)
1201 (%)	9 (9.6)	6 (10.2)	3 (8.6)	33 (9.0)
1202 (%)	0 (0.0)	0 (0.0)	0 (0.0)	13 (3.5)
1301 (%)	1 (1.1)	1 (1.7)	0 (0.0)	1 (0.3)
1302 (%)	3 (3.2)	1 (1.7)	2 (5.7)	49 (13.4)
1403 (%)	2 (2.1)	0 (0.0)	2 (5.7)	8 (2.2)
1405 (%)	3 (3.2)	2 (3.4)	1 (2.9)	14 (3.8)
1406 (%)	3 (3.2)	2 (3.4)	1 (2.9)	8 (2.2)
1454 (%)	2 (2.1)	2 (3.4)	0 (0.0)	19 (5.2)
1501 (%)	24 (25.5)	20 (33.9)*[d]	4 (11.4)	60 (16.4)
1502 (%)	14 (14.9)	8 (13.6)	6 (17.1)	80 (21.8)
1601 (%)	0 (0.0)	0 (0.0)	0 (0.0)	1 (0.3)
1602 (%)	0 (0.0)	0 (0.0)	0 (0.0)	3 (0.8)

*[a]Compared with HCs, $p^{corr} = 0.0196$, OR = 2.217, 95% CI = 1.389–3.539.
*[b]Compared with HCs, $p^{corr} = 0.0056$, OR = 3.660, 95% CI = 1.802–7.431.
*[c]Compared with HCs, $p^{corr} = 0.0084$, OR = 0.279, 95% CI = 0.135–0.575.
*[d]Compared with HCs, $p^{corr} = 0.0392$, OR = 2.624, 95% CI 1.432–4.809.
p^{uncorr} was corrected by multiplying the value by 28 to calculate p^{corr}.
CI, confidence interval; CSF, cerebrospinal fluid; HCs, healthy controls; MS, multiple sclerosis; OR, odds ratio; p^{corr}, corrected p value.
doi:10.1371/journal.pone.0095367.t002

patients showed a significantly higher frequency of the *DRB1*0405* allele ($p^{corr} = 0.0056$, OR = 3.660, 95% CI = 1.802–7.431) (Table 2). The frequency of CSF IgG abnormality was 83.3% in MS patients with the *DRB1*1501* allele compared with 52.4% in MS patients with the *DRB1*0405* allele (p = 0.0119).

Relationships between CSF IgG abnormality status and common infectious agents

Anti-*C. pneumoniae* IgG antibodies were significantly more frequently detected in MS patients with CSF IgG abnormality than in those without CSF IgG abnormality (p = 0.0119) (Table 3), although there was no difference in the frequency of anti-*C. pneumoniae* IgG antibodies between HCs and total MS patients. Compared with HCs, anti-*H. pylori* IgG antibodies were detected significantly less frequently in the total MS patients (p = 0.0451) and CSF IgG abnormality-negative MS patients (p = 0.0474) (Table 3). There was no difference in the frequency of anti-*H. pylori* IgG antibodies between CSF IgG abnormality-positive and abnormality-negative patients. Neither the anti-EBNA nor anti-VZV antibody positivity rates differed significantly among the groups. Among the common infectious agents, only the *H. pylori* infection rate decreased successively with advancing year of birth (p = 0.0014) (Figure 2).

Discussion

The main new findings of the present study are as follows: (1) compared with HCs, CSF IgG abnormality-positive MS patients had a significantly higher frequency of *HLA-DRB1*1501*, whereas CSF IgG abnormality-negative MS patients had a significantly higher frequency of *HLA-DRB1*0405*; (2) CSF IgG abnormality-positive MS patients had a significantly higher frequency of anti-*C. pneumoniae* IgG antibodies compared with abnormality-negative MS patients, although there was no difference in the frequency of anti-*C. pneumoniae* IgG antibodies between HCs and total MS patients; and (3) compared with HCs, the frequencies of anti-*H.*

Table 3. Comparisons of the frequencies of antibodies against common infectious agents.

	MS	CSF IgG abnormality (+)	CSF IgG abnormality (−)	HCs
Chlamydia pneumoniae	56/90 (62.22%)	42/58 (72.4%)*	14/32 (43.8%)*	92/156 (58.97%)
Helicobacter pylori	26/90 (28.89%)**	19/58 (32.8%)	7/32(21.9%)***	74/177 (41.81%)**, ***
EBV	86/90 (95.56%)	56/58 (96.6%)	30/32 (93.8%)	143/156 (91.67%)
VZV	89/90 (98.89%)	57/58 (98.3%)	32/32 (100%)	153/156 (98.08%)

*p = 0.0119, compared with IgG abnormality (−) MS patients.
**p = 0.0451, compared with HCs.
***p = 0.0474, compared with HCs.
*,**,***Significant difference between the linked values ($p<0.05$).
The age of the patients during examination did not differ significantly among HCs and MS patients, regardless of the presence or absence of IgG abnormality (mean ± SD in years: 37.21±12.54 for MS; 36.19±11.36 for IgG abnormality-positive MS; 39.00±14.39 for IgG abnormality-negative MS; and 38.93±12.11 for HCs).
CSF, cerebrospinal fluid; EBV, Epstein-Barr virus; HCs, healthy controls; MS, multiple sclerosis; p^{corr}, corrected p value; VZV, varicella zoster virus.
doi:10.1371/journal.pone.0095367.t003

pylori IgG antibodies were lower, especially in CSF IgG abnormality-negative MS patients.

The number of enrolled MS patients was not large because of the relative rarity of the disease in the Japanese population, and this could lead to partly inconclusive results. However, this study is the first to investigate the influence of *HLA-DRB1* alleles on CSF IgG abnormality in MS patients in Japan when NMO and NMOSD patients were excluded, and is the only study to simultaneously investigate the influence of common infectious agents as environmental risk or protective factors. The ELISAs used in the present study have reasonably high sensitivity and specificity [37,38], although *H. pylori* and *C. pneumoniae* infections should be confirmed by methods other than ELISA in future studies.

In the present study, we demonstrated that the presence or absence of CSF IgG abnormality did not predict the prognosis for the disease course of Japanese MS patients, consistent with relatively larger studies in Western countries and a Japanese study in Hokkaido, the northernmost island of Japan [18,26–28]. Additionally, the frequency of CSF IgG abnormality did not differ according to the clinical subtypes of MS.

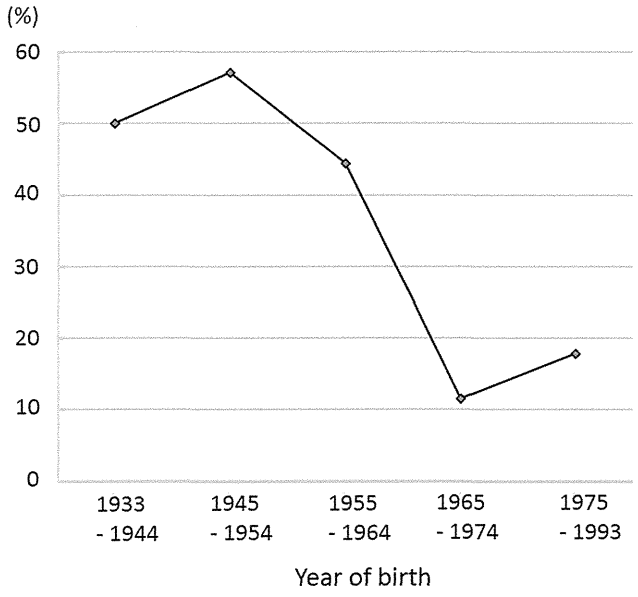

Figure 2. Proportions of patients with *Helicobacter pylori* infection by year of birth. Among the MS patients, the proportion of patients with *H. pylori* decreased markedly in those born after 1965. MS, multiple sclerosis.
doi:10.1371/journal.pone.0095367.g002

In CSF IgG abnormality-positive MS patients, the only significant difference was the more frequent presence of brain MRI lesions meeting the Barkhof criteria compared with CSF IgG abnormality-negative MS patients. Carriage of *HLA-DRB1*1501* was associated with an approximately 2.6-fold increased risk for CSF IgG abnormality-positive MS. This is in line with previous findings demonstrating that *DRB1*15* is associated with OB-positive MS in Swedish patients [22], Spanish patients [23], and the Japanese population of Hokkaido [19]. Taken together, in this subpopulation, MS was associated with greater brain MRI lesion loads, presence of the *HLA-DRB1*1501* allele, and increased humoral immune responses in CSF in Japanese. These features also resemble those of MS in Western people [39,40]. Therefore, this subgroup of Japanese patients represents a "Western" type of MS in terms of CSF, neuroimaging, and genetic characteristics. In Caucasians, the presence of the *DRB1*1501* allele promotes the development of more T2 lesions [41] and intrathecal IgG synthesis [42]. Similar biological mechanisms may occur in Asian patients.

In CSF IgG abnormality-negative MS patients, *HLA-DRB1*0405* showed an approximately 3.6-fold increased risk for the condition. In this subgroup, MS was characterized by lower MRI brain lesion loads. This is in line with previous findings that *DRB1*04* is associated with OB-negative MS in Swedish patients [22] and the Japanese population of Hokkaido [19]. The low frequency of CSF IgG abnormality is a unique feature in Japanese MS patients, compared with Western MS patients [17,20]. *DRB1*0405* is present in a relatively minor population of Caucasian MS patients [22], while about 60% of MS patients in Northern Europe are positive for *HLA-DRB1*15*, compared with 30% of HCs [43]. The relatively high frequency of Japanese MS patients carrying the *DRB1*0405* allele may be partly responsible for the low prevalence of CSF IgG abnormality in Japanese MS patients. According to the fourth nationwide survey of MS in Japanese people, the most common type of MS had neither Barkhof brain lesions nor longitudinally extensive spinal cord lesions [44]. Hence, CSF IgG abnormality-negative Japanese MS could be a unique subgroup of MS in terms of CSF, neuroimaging, and genetic characteristics. Kuenz et al. [45] showed that CSF B cells were correlated with paraclinical markers such as high numbers of MRI T2 lesions, intrathecal IgG synthesis, and intrathecal production of MMP-9 and B cell chemokine CxCL-13. These findings may suggest that distinct immune mechanisms between IgG abnormality-positive and abnormality-negative

patients lead to the differences in their CSF and neuroimaging characteristics.

In the present study, we showed that *C. pneumoniae* infection was higher in CSF IgG abnormality-positive MS patients than in abnormality-negative MS patients. The mechanism for the abnormal intrathecal IgG synthesis in MS patients infected with *C. pneumoniae* could be molecular mimicry [46], i.e., cross-reactivity of humoral immune responses against *C-pneumoniae* antigens and CNS self-antigens. To date, however, OBs have not been found to react highly specifically with any microbial antigens or self-antigens. It is possible that anti-*C. pneumoniae* IgG antibodies directly confer CSF IgG abnormality in MS patients. In general, however, CSF anti-*C. pneumoniae* IgG antibodies are only found in a small portion of MS patients, with no differences between MS and controls [47–50]. These findings suggest that *C. pneumoniae* infection may indirectly modify the intrathecal humoral immune functions, leading to CSF IgG abnormality in patients with MS.

It is interesting to note that CSF IgG abnormality-negative MS patients had a lower frequency of *H. pylori* infection compared with HCs in addition to a lower frequency of *C. pneumoniae* infection compared with CSF IgG abnormality-positive MS patients. To date, there have been no reports focusing on the association between CSF IgG abnormality and *H. pylori* infection, and there has been no firm evidence of molecular mimicry between human myelin antigens and *H. pylori*. Therefore, it is extremely difficult to speculate on the mechanism by which *H. pylori* infection differentially affects MS subpopulations with and without CSF IgG abnormality. However, these observations extend our previous finding that the rates of *H. pylori* infection, which occurs in the infantile period and reflects sanitary conditions in younger ages, were lower in Japanese MS patients, compared with HCs [12]. Additionally, the proportion of patients with *H. pylori* infection decreased successively with advancing year of birth. These findings collectively suggest that CSF IgG abnormality-negative MS patients may have grown up in a relatively clean environment. It is possible that a clean environment at younger ages may confer CSF IgG abnormality-negative MS. We previously reported that *HLA-DRB1*0405*-positive MS showing a lower frequency of CSF IgG abnormality is increasing in the younger Japanese population [7]. Thus, a modernized clean environment may potentiate susceptibility to this subtype of MS without CSF IgG abnormality in *HLA-DRB1*0405* carriers. This possibility should be investigated in future large-scale studies.

In conclusion, *DRB1*1501* and *C. pneumoniae* infection confer CSF IgG abnormality, while *DRB1*0405* and *H. pylori* infection are positively and negatively associated with CSF IgG abnormality-negative MS, respectively, suggesting that genetic and environmental factors differentially contribute to MS susceptibility according to the CSF IgG abnormality status.

Author Contributions

Conceived and designed the experiments: SY JK. Performed the experiments: SY NI TM YK SS. Analyzed the data: SY. Contributed reagents/materials/analysis tools: SY NI TM KM SS YK HO JK. Wrote the paper: SY JK.

References

1. Compston A, Coles A (2008) Multiple sclerosis. Lancet 372: 1502–1517
2. Ebers GC (2008) Environmental factors and multiple sclerosis. Lancet Neurol 7: 268–277.
3. Sweer S, Hellenthal G, Pirinen M, Spencer CC, Patsopoulos NA, et al. (2011) Genetic risk and a primary role for cell-mediated immune mechanisms in multiple sclerosis. Nature 476(7359): 214–219.
4. Kira J, Kanai T, Nishimura Y, Yamasaki K, Matsushita S, et al. (1996) Western versus Asian types of multiple sclerosis: immunogenetically and clinically distinct disorders. Ann Neurol 40: 569–574.
5. Yamasaki K, Horiuchi I, Minohara M, Kawano Y, Ohyagi Y, et al. (1999) HLA-DPB1*0501-associated opticospinal multiple sclerosis: clinical, neuroimaging and immunogenetic studies. Brain 122:1689–1696.
6. Ono T, Zambenedetti MR, Yamasaki K, Kawano Y, Kamikawaji N, et al. (1998) Molecular analysis of HLA class I (HLA-A and -B) and HLA class II (HLA-DRB1) genes in Japanese patients with multiple sclerosis (Western type and Asian type). Tissue Antigens 52: 539–542.
7. Yoshimura S, Isobe N, Yonekawa T, Matsushita T, Masaki K, et al. (2012) South Japan Multiple Sclerosis Genetics Consortium: genetic and infectious profiles of Japanese multiple sclerosis patients. PLoS ONE 7: e48592.
8. Levin LI, Munger KL, O'Reilly EJ, Falk KI, Ascherio A (2010) Primary infection with the Epstein-Barr virus and risk of multiple sclerosis. Ann Neurol 67: 824–830.
9. Handel AE, Giovannoni G, Ebers GC, Ramagopalan SV (2010) Environmental factors and their timing in adult-onset multiple sclerosis. Nat Rev Neurol 6: 156–166.
10. Sriram S, Stratton CW, Yao S, Tharp A, Ding L, et al. (1999) Chlamydia pneumoniae infection of the central nervous system in multiple sclerosis. Ann Neurol 46: 6–14.
11. Bagos PG, Nikolopoulos G, Ioannidis A (2006) Chlamydia pneumoniae infection and the risk of multiple sclerosis: a meta-analysis. Mult Scler 12: 397–411.
12. Li W, Minohara M, Su JJ, Matsuoka T, Osoegawa M, et al. (2007) Helicobacter pylori infection is a potential protective factor against conventional multiple sclerosis in the Japanese population. J Neuroimmunol 184: 227–331.
13. Li W, Minohara M, Piao H, Matsushita T, Masaki K, et al. (2009). Association of anti-Helicobacter pylori neutrophil-activating protein antibody response with anti-aquaporin-4 autoimmunity in Japanese patients with multiple sclerosis and neuromyelitis optica. Mult Scler 15: 1411–1421.
14. Yoshimura S, Isobe N, Matsushita T, Yonekawa T, Masaki K, et al. (2013) Distinct genetic and infectious profiles in Japanese neuromyelitis optica patients according to anti-aquaporin 4 antibody status. J Neurol Neurosurg Psychiatry 84: 29–34.
15. Link H, Huang YM (2006) Oligoclonal bands in multiple sclerosis cerebrospinal fluid: an update on methodology and clinical usefulness. J Neuroimmunol180: 17–28.
16. Lechner-Scott J, Spencer B, de Malmanche T, Attia J, Fitzgerald M, et al. (2012) The frequency of CSF oligoclonal banding in multiple sclerosis increases with latitude. Mult Scler 18: 974–982.
17. Kira J (2003) Multiple sclerosis in the Japanese population. Lancet Neurol 2: 117–127.
18. Fukazawa T, Kikuchi S, Sasaki H, Hamada K, Hamada T, et al. (1998). The significance of oligoclonal bands in multiple sclerosis in Japan: relevance of immunogenetic backgrounds. J Neurol Sci 158: 209–214.
19. Kikuchi S, Fukazawa T, Niino M, Yabe I, Miyagishi R, et al. (2003) HLA-related subpopulations of MS in Japanese with and without oligoclonal IgG bands. Neurology 60: 647–651.
20. Nakashima I, Fujihara K, Sato S, Itoyama Y (2005) Oligoclonal IgG bands in Japanese patients with multiple sclerosis. A comparative study between isoelectric focusing with IgG immunofixation and high-resolution agarose gel electrophoresis. J Neuroimmunol. 159: 133–136.
21. Siritho S, Prayoonwiwat N (2007) A retrospective study of multiple sclerosis in Siriraj Hospital, Bankok, Thailand. Can J Neurol Sci 34: 99–104.
22. Imrell K, Landtblom AM, Hillert J, Masterman T (2006) Multiple sclerosis with and without CSF bands: clinically indistinguishable but immunogenetically distinct. Neurology 67: 1062–1064.
23. Romero-Pinel L, Martínez-Yélamos S, Bau L, Matas E, Gubieras L, et al. (2011) Association of HLA-DRB1*15 allele and CSF oligoclonal bands in a Spanish multiple sclerosis cohort. Eur J Neurol 8: 1258–1262.
24. Stendahl-Brodin L, Link H (1980) Relation between benign course of multiple sclerosis and low-grade humoral immune response in cerebrospinal fluid. J Neurol Neurosurg Psychiatry 43: 102–105.
25. Zeman AZ, Kidd D, McLean BN, Kelly MA, Francis DA, et al. (1996) A study of oligoclonal band negative multiple sclerosis. J Neurol Neurosurg Psychiatry 60: 27–30.
26. Koch M, Heersema D, Mostert J, Teelken A, De Keyser J (2007) Cerebrospinal fluid oligoclonal bands and progression of disability in multiple sclerosis. Eur J Neurol 14: 797–800.
27. Siritho S, Freedman MS (2009) The prognostic significance of cerebrospinal fluid in multiple sclerosis. J Neurol Sci 279: 21–25.
28. Lourenco P, Shirani A, Saeedi J, Oger J, Schreiber WE, et al. (2013) Oligoclonal bands and cerebrospinal fluid markers in multiple sclerosis: associations with disease course and progression. Mult Scler 19: 577–584
29. Nakashima I, Fujihara K, Misu T, Fujimori J, Sato S, et al. (2002) A comparative study of Japanese multiple sclerosis patients with and without oligoclonal IgG bands. Mult Scler 8: 459–462.
30. Polman CH, Reingold SC, Edan G, Filippi M, Hartung HP, et al. (2005) Diagnostic criteria for multiple sclerosis: 2005 revisions to the "McDonald Criteria". Ann Neurol 58: 840–846.

31. Wingerchuk DM, Lennon VA, Pittock SJ, Lucchinetti CF, Weinshenker BG (2006) Revised diagnostic criteria for neuromyelitis optica. Neurology 66: 1485–1489.
32. Kurtzke JF (1983) Rating neurologic impairment in multiple sclerosis: an expanded disability status scale (EDSS). Neurology 33: 1444–1452.
33. Poser S, Ritter G, Bauer HJ, Grosse-Wilde H, Kuwert EK, et al. (1981) HLA-antigens and the prognosis of multiple sclerosis. J Neurol 225: 219–221.
34. Barkhof F, Filippi M, Miller DH, Scheltens P, Campi A, et al. (1997) Comparison of MRI criteria at first presentation to predict conversion to clinically definite multiple sclerosis. Brain 120: 2059–2069.
35. Matsuoka T, Matsushita T, Osoegawa M, Ochi H, Kawano Y, et al. (2008) Heterogeneity and continuum of multiple sclerosis in Japanese according to magnetic resonance imaging findings. J Neurol Sci 266: 115–125.
36. Isobe N, Yonekawa T, Matsushita T, Kawano Y, Masaki K, (2012) Quantitative assays for anti-aquaporin-4 antibody with subclass analysis in neuromyelitis optica. Mult Scler 18: 1541–1551
37. Laheij RJ, Straatman H, Jansen JB, Verbeek AL (1998) Evaluation of commercially available Helicobacter pylori serology kits: a review. J Clin Microbiol 36: 2803–2809.
38. Hermann C, Graf K, Groh A, Straube E, Hartung T (2002) Comparison of eleven commercial tests for Chlamydia pneumoniaespecific immunoglobulin G in asymptomatic healthy individuals. J Clin Microbiol 40: 1603–1609.
39. Wu JS, Qiu W, Castley A, James I, Joseph J, et al. (2010) Presence of CSF oligoclonal bands (OCB) is associated with the HLA-DRB1 genotype in a West Australian multiple sclerosis cohort. J Neurol Sci 288: 63–67.
40. Romero-Pinel L, Martínez-Yélamos S, Bau L, Matas E, Gubieras L, et al. (2011) Association of HLA-DRB1*15 allele and CSF oligoclonal bands in a Spanish multiple sclerosis cohort. Eur J Neurol 18:1258–1262.
41. Okuda DT, Srinivasan R, Oksenberg JR, Goodin DS, Baranzini SE, et al. (2009). Genotype-phenotype correlations in multiple sclerosis: HLA genes influence disease severity inferred by 1HMR spectroscopy and MRI measures. Brain 132: 250–259.
42. Sellebjerg F, Jensen J, Madsen HO, Svejgaard A (2000) HLA DRB1*1501 and intrathecal inflammation in multiple sclerosis. Tissue Antigens 55: 312–318.
43. Masterman T, Ligers A, Olsson T, Andersson M, Olerup O, et al. (2000) HLA-DR15 is associated with lower age at onset in multiple sclerosis. Ann Neurol 48: 211–219.
44. Ishizu T, Kira J, Osoegawa M, Fukazawa T, Kikuchi S, et al. (2009) Research Committee of Neuroimmunological Diseases: Heterogeneity and continuum of multiple sclerosis phenotypes in Japanese according to the results of the fourth nationwide survey. J Neurol Sci 280: 22–28.
45. Kuenz B, Lutterotti A, Ehling R, Gneiss C, Haemmerle M, et al. (2008) Cerebrospinal fluid B cells correlate with early brain inflammation in multiple sclerosis. PLoS One. 3: e2559.
46. Kamradt T, Goggel R, Erb KJ (2005) Induction, exacerbation and inhibition of allergic and autoimmune diseases by infection. Trend Immun 26: 260–267.
47. Layh-Schmitt G, Bendl C, Hildt U, Dong-Si T, Jüttler E, et al. (2000) Evidence for infection with Chlamydia pneumoniae in a subgroup of patients with multiple sclerosis. Ann Neurol 47: 652–655.
48. Derfuss T, Gürkov R, Then Bergh F, Goebels N, Hartmann M, et al. (2001) Intrathecal antibody production against Chlamydia pneumoniae in multiple sclerosis is part of a polyspecific immune response. Brain 124: 1325–1335.
49. Saiz A, Marcos MA, Graus F, Vidal J, Jimenez de Anta MT (2001) No evidence of CNS infection with Chlamydia pneumoniae in patients with multiple sclerosis. J Neurol 248: 617–618.
50. Sotgiu S, Piana A, Pugliatti M, Sotgiu A, Deiana GA, et al. (2001) Chlamydia pneumoniae in the cerebrospinal fluid of patients with multiple sclerosis and neurological controls. Mult Scler 7: 371–374.

Identification of Independent Susceptible and Protective HLA Alleles in Japanese Autoimmune Thyroid Disease and Their Epistasis

Sho Ueda,* Daisuke Oryoji,* Ken Yamamoto,* Jaeduk Yoshimura Noh, Ken Okamura, Mitsuhiko Noda, Koichi Kashiwase, Yuka Kosuga, Kenichi Sekiya, Kaori Inoue, Hisakata Yamada, Akiko Oyamada, Yasuharu Nishimura, Yasunobu Yoshikai, Koichi Ito, and Takehiko Sasazuki

Institute for Advanced Study (S.U., D.O., T.S.), Division of Genome Analysis (K.Y.), Medical Institute of Bioregulation, Department of Medicine and Clinical Science (K.O.), Graduate School of Medicine, and Division of Host Defense (H.Y., A.O., Y.Y.), Medical Institute of Bioregulation, Kyushu University, Kyushu University, Higashi-ku, Fukuoka 812-8582, Japan; Ito Hospital (J.Y.N., Y.K., K.S., K.I.), Shibuya-ku, Tokyo 150-8308, Japan; Department of Diabetes and Metabolic Medicine (M.N., K.I.), National Center for Global Health and Medicine, Shinjuku-ku, Tokyo 16-8655, Japan; Department of Laboratory (K.K.), Japanese Red Cross Tokyo Blood Center, Koto-ku, Tokyo 135-8639, Japan; and Department of Immunogenetics (Y.N.), Graduate School of Medical Sciences, Kumamoto University, Chuo-ku, Kumamoto 860-8556, Japan

Background: Autoimmune thyroid disease (AITD) includes Graves disease (GD) and Hashimoto thyroiditis (HT), which partially share immunological features. Determining the genetic basis that distinguishes GD and HT is a key to understanding the differences between these 2 related diseases.

Aim: The aims of this study were to identify HLA antigens that can explain the immunopathological difference between GD and HT and to elucidate epistatic interactions between protective and susceptible *HLA* alleles, which can delineate the distinct function of *HLA* in AITD etiology.

Design: We genotyped 991 patients with AITD (547 patients with GD and 444 patients with HT) and 481 control subjects at the *HLA-A*, *HLA-C*, *HLA-B*, *DRB1*, *DQB1*, and *DPB1* loci. A direct comparison of HLA antigen frequencies between GD and HT was performed. We further analyzed an epistatic interaction between the susceptible and protective *HLA* alleles in the development of GD and HT.

Results: We identified 4 and 2 susceptible HLA molecules primarily associated with GD and HT, respectively, *HLA-B*35:01*, *HLA-B*46:01*, *HLA-DRB1*14:03*, and *HLA-DPB1*05:01* for GD and *HLA-A*02:07* and *HLA-DRB4* for HT. In a direct comparison between GD and HT, we identified GD-specific susceptible class II molecules, HLA-DP5 (*HLA-DPB1*05:01*; $Pc = 1.0 \times 10^{-9}$) and HLA-DR14 (*HLA-DRB*14:03*; $Pc = .0018$). In contrast, *HLA* components on 3 common haplotypes in Japanese showed significant protective effects against the development of GD and HT (*HLA-A*24:02-C*12:02-B*52:01-DRB1*15:02-DQB1*06:01-DPB1*09:01* and *HLA-A*24:02-C*07:02-B*07:02-DRB1*01:01-DQB1*05:01-DPB1*04:02* haplotypes for GD and *HLA-A*33:03-C*14:03-B*44:03-DRB1*13:02-DQB1*06:04-DPB1*04:01* haplotype for GD and HT). Interestingly, the representative protective HLA, HLA-DR13 (*HLA-DRB1*13:02*), was epistatic to susceptible HLA-DP5 in controlling the development of GD.

Conclusion: We show that HLA exerts a dual function, susceptibility and resistance, in controlling the development of GD and HT. We also show that the protective HLA allele is partially epistatic to the susceptible HLA allele in GD. **(*J Clin Endocrinol Metab* 99: E379–E383, 2014)**

ISSN Print 0021-972X ISSN Online 1945-7197
Printed in U.S.A.

Received July 12, 2013. Accepted November 11, 2013.
First Published Online November 27, 2013

* S.U., D.O., and K.Y. contributed equally to the study.

Abbreviations: AITD, autoimmune thyroid disease; CI, confidence interval; GD, Graves disease; HT, Hashimoto thyroiditis; LD, linkage disequilibrium; OR, odds ratio.

Autoimmune thyroid disease (AITD), including Graves disease (GD) and Hashimoto thyroiditis (HT), is one of the most common autoimmune diseases (1, 2). The result of AITD is 2 clinically opposing syndromes: GD is characterized by hyperthyroidism due to the production of agonistic antithyroid–stimulating hormone receptor antibody, and HT is characterized by hypothyroidism due to a cell-mediated immune response to the thyroid gland (3). It is evident that the etiology of AITD involves both genetic and environmental factors (4, 5). The facts that GD and HT clustered in the same family and that GD progressed into HT in an individual patient might suggest that GD and HT share the same genetic factors (3).

Among the genetic factors, *HLA* genes show the strongest association with GD (6, 7), and both predisposing and protective effects of HLA in GD and HT have been reported (8–17). However, the extensive allelic variations and strong linkage disequilibrium (LD) among the HLA alleles have confounded attempts to clearly identify the actual susceptible and protective alleles in AITD. Although a comparison of the HLA class II association seen in GD and HT in Caucasians has been reported (8), a direct comparison of HLA association between GD and HT in the Japanese AITD population has not been undertaken. Furthermore, an analysis of epistatic interactions between protective and susceptible *HLA* alleles to delineate the distinct function of *HLA* in AITD etiology has not been performed.

Here, we conducted a case-control study of 991 unrelated Japanese patients with AITD (547 patients with GD and 444 patients with HT) and 481 control subjects, comparing 81 *HLA* alleles at 7 loci, and performed a direct comparison of HLA antigen frequencies between GD and HT to elucidate the immunogenetic differences and overlaps between GD and HT. Furthermore, to gain insight into the immunogenetic roles of HLA in the etiology of AITD, we analyzed an epistatic interaction between susceptible and protective *HLA* alleles in the development of GD and HT.

Subjects and Methods

Subjects

Unrelated Japanese patients with GD and HT and healthy control subjects (547, 444, and 481 samples, respectively) were enrolled. All recruiting centers used standard clinical criteria to diagnose AITD (see Supplementary Method published on The Endocrine Society's Journals Online web site at http://jcem.endojournals.org.). Documented informed consent was obtained from each participant according to the Declaration of Helsinki. This study was also approved by the Ethics Committee at Kyushu University, Fukuoka, Japan.

HLA genotyping

We determined *HLA-A*, *HLA-C*, *HLA-B*, *HLA-DRB1*, *HLA-DQB1*, and *HLA-DPB1* genotypes using the Luminex assay system (Luminex Corporation) and HLA typing kits (Wakunaga). Alleles of the *HLA-DRB3/4/5* loci were deduced from the *HLA-DRB1* alleles through the perfect LD between them. We observed a total of 151 alleles (*HLA-A*, 24; *HLA-C*, 20; *HLA-B*, 42; *HLA-DRB1*, 32; *HLA-DQB1*, 15; *HLA-DPB1*, 14; and *HLA-DRB3/4/5*, 4).

Statistical analysis

The *P* value and odds ratios (ORs) were computed using PLINK version 1.07 software (18). We tested common alleles with a frequency higher than 1% in either case patients or control subjects (total allele number was 81). The frequencies of the most frequent haplotypes were determined with the maximum likelihood method using Haploview version 4.2 software (19). The data were compared using χ^2 analysis and logistic regression analysis for conditional analysis to determine the primarily associated HLA antigen using other HLA alleles that are in LD with each other as covariables. *P* values were corrected for the number of different alleles tested (*Pc*) using the Bonferroni method, and significance was determined at $Pc < .05$.

Results

Identification of susceptible and protective HLA antigens for GD

*HLA-C*03:03*, *HLA-B*35:01*, *HLA-B*46:01*, *HLA-DRB1*14:03*, and *HLA-DPB1*05:01* showed positive associations with GD ($Pc < .05$) (Table 1). Consistent with LD among *HLA* alleles, we observed that the association of *HLA-C*03:03* with GD did not keep significance in the conditional analysis with adjustment for *HLA-B*35:01* (Supplemental Table 1). Thus, we identified 2 HLA class I (*HLA-B*35:01* and *HLA-B*46:01*) and 2 class II antigens (*HLA-DRB1*14:03* and *HLA-DPB1*05:01*) as primary GD-susceptible HLA antigens in this analysis.

A total of 14 antigens showed protective effects against the development of GD significantly ($Pc < .05$) (Table 1). It should be noted that all of these alleles were components of the 3 most common *HLA* haplotypes in Japanese populations: *HLA-A*24:02*, *HLA-C*12:02*, *HLA-B*52:01*, *HLA-DRB1*15:02*, and *HLA-DPB1*09:01* are on the most common haplotype (designated as HP-1; *A*24:02-C*12:02-B*52:01-DRB1*15:02-DQB1*06:01-DPB1*09:01*); *HLA-A*33:03*, *HLA-C*14:03*, *HLA-B*44:03*, *HLA-DRB1*13:02*, *HLA-DQB1*06:04*, and *HLA-DPB1*04:01* are on the second most common haplotype (designated as HP-2; *A*33:03-C*14:03-B*44:03-DRB1*13:02-DQB1*06:04-DPB1*04:01*); and *HLA-B*07:02*, *HLA-DRB1*01:01*, and *HLA-DQB1*05:01* are on the third most common haplotype (designated as HP-3; *A*24:02-C*07:02-B*07:02-DRB1*01:01-DQB1*05:01-DPB1*04:02*). The conditional analysis revealed that HLA-DR15 (*HLA-*

Table 1. List of *HLA* Alleles Associated with GD and HT

	Antigen Frequency (Number)				GD vs Control			HT vs Control			GD vs HT	
HLA	GD	HT	AITD	Control	OR (95% CI)	*P*	*Pc*	OR (95% CI)	*P*	*Pc*	*P*	*Pc*
*A*02:07*	0.10 (55)	0.17 (75)	0.13 (130)	0.06 (27)	1.88 (1.17–3.03)	.0096	NS	3.42 (2.16–5.42)	1.7×10^{-7}	1.4×10^{-5}	.0017	NS
*A*24:02*	0.50 (276)	0.58 (256)	0.54 (532)	0.62 (299)	0.62 (0.48–0.80)	1.7×10^{-4}	.014	0.83 (0.64–1.08)	.16	NS	.024	NS
*A*33:03*	0.07 (37)	0.10 (45)	0.08 (82)	0.17 (84)	0.34 (0.23–0.52)	2.8×10^{-7}	2.4×10^{-5}	0.53 (0.36–0.79)	.0015	NS	.057	NS
*C*03:03*	0.30 (165)	0.23 (104)	0.27 (269)	0.19 (91)	1.85 (1.38–2.47)	3.9×10^{-5}	.0033	1.31 (0.95–1.80)	.097	NS	.018	NS
*C*12:02*	0.14 (74)	0.19 (84)	0.16 (158)	0.22 (107)	0.55 (0.39–0.76)	2.7×10^{-4}	.023	0.81 (0.59–1.12)	.21	NS	.022	NS
*C*14:03*	0.05 (27)	0.08 (36)	0.06 (63)	0.17 (80)	0.26 (0.16–0.41)	6.4×10^{-9}	5.5×10^{-7}	0.44 (0.29–0.67)	1.2×10^{-4}	.0098	.044	NS
*B*07:02*	0.06 (31)	0.09 (40)	0.07 (71)	0.14 (66)	0.38 (0.24–0.59)	1.9×10^{-5}	.0016	0.62 (0.41–0.94)	.026	NS	.044	NS
*B*35:01*	0.23 (128)	0.19 (83)	0.21 (211)	0.11 (54)	2.42 (1.71–3.41)	5.6×10^{-7}	4.8×10^{-5}	1.82 (1.26–2.63)	.0016	NS	.072	NS
*B*44:03*	0.05 (28)	0.08 (34)	0.06 (62)	0.17 (80)	0.27 (0.17–0.42)	1.2×10^{-8}	1.0×10^{-6}	0.42 (0.27–0.64)	5.0×10^{-5}	.0041	.1	NS
*B*46:01*	0.17 (95)	0.20 (89)	0.19 (184)	0.09 (43)	2.14 (1.46–3.14)	1.0×10^{-4}	.0085	2.55 (1.73–3.77)	2.5×10^{-6}	2.1×10^{-4}	.28	NS
*B*52:01*	0.13 (72)	0.19 (83)	0.16 (155)	0.22 (108)	0.52 (0.38–0.73)	1.1×10^{-4}	.0092	0.79 (0.58–1.09)	.16	NS	.018	NS
*DRB1*01:01*	0.07 (36)	0.09 (39)	0.08 (75)	0.14 (67)	0.44 (0.28–0.67)	1.3×10^{-4}	.011	0.60 (0.39–0.90)	.015	NS	.19	NS
*DRB1*08:03*	0.21 (113)	0.26 (117)	0.23 (230)	0.16 (75)	1.41 (1.02–1.94)	.037	NS	1.94 (1.40–2.68)	6.5×10^{-5}	.0053	.035	NS
*DRB1*13:02*	0.06 (33)	0.05 (21)	0.05 (54)	0.16 (78)	0.33 (0.22–0.51)	4.2×10^{-7}	3.6×10^{-5}	0.26 (0.16–0.42)	1.0×10^{-7}	8.2×10^{-6}	.37	NS
*DRB1*14:03*	0.08 (46)	0.02 (7)	0.05 (53)	0.03 (14)	3.06 (1.66–5.65)	3.3×10^{-4}	.028	0.53 (0.21–1.34)	.18	NS	2.1×10^{-5}	.0018
*DRB1*15:02*	0.09 (50)	0.15 (66)	0.12 (116)	0.22 (108)	0.35 (0.24–0.50)	9.6×10^{-9}	8.2×10^{-7}	0.60 (0.43–0.85)	.0034	NS	.0057	NS
DRB3	0.35 (192)	0.29 (128)	0.32 (320)	0.41 (197)	0.78 (0.61–1.00)	.054	NS	0.58 (0.44–0.77)	1.2×10^{-4}	.0098	.036	NS
DRB4	0.69 (380)	0.75 (335)	0.72 (715)	0.63 (301)	1.36 (1.05–1.76)	0.02	NS	1.84 (1.38–2.44)	2.7×10^{-5}	.0022	.037	NS
*DQB1*05:01*	0.07 (38)	0.10 (43)	0.08 (81)	0.14 (68)	0.45 (0.30–0.69)	2.1×10^{-4}	.018	0.65 (0.43–0.98)	.038	NS	.12	NS
*DQB1*06:04*	0.06 (32)	0.04 (19)	0.05 (51)	0.15 (72)	0.35 (0.23–0.55)	2.9×10^{-6}	2.4×10^{-4}	0.25 (0.15–0.43)	2.9×10^{-7}	2.4×10^{-5}	.27	NS
*DPB1*04:01*	0.06 (31)	0.05 (21)	0.05 (52)	0.14 (66)	0.38 (0.24–0.59)	1.9×10^{-5}	.0016	0.31 (0.19–0.52)	7.5×10^{-6}	6.2×10^{-4}	.51	NS
*DPB1*05:01*	0.82 (450)	0.63 (279)	0.74 (729)	0.59 (286)	3.16 (2.38–4.21)	2.4×10^{-15}	2.1×10^{-13}	1.15 (0.88–1.50)	.29	NS	1.2×10^{-11}	1.0×10^{-9}
*DPB1*09:01*	0.09 (50)	0.14 (61)	0.11 (111)	0.20 (97)	0.40 (0.28–0.57)	8.4×10^{-7}	7.1×10^{-5}	0.63 (0.44–0.89)	.0098	NS	.023	NS

Abbreviation: NS, not significant. The numbers of patients with GD and HT and control subjects were 547, 444, and 481, respectively. The corrected *P* values (*Pc*) were obtained with the Bonferroni method (number of tests = 85).

*DRB1*15:02*; OR = 0.35, 95% confidence interval [CI] = 0.24–0.50, $Pc = 8.2 \times 10^{-7}$) on HP-1 showed a primary protective association with GD (Supplemental Table 2). Regarding HP-2 and HP-3, we could not pinpoint primarily associated antigens with conditional analysis due to strong LD. However, a haplotype-based association study confirmed the significant protective association of HP-2 and HP-3 with GD (Supplemental Table 3). It is possible that multiple alleles on HP-2 or HP-3 control the resistance to GD.

Identification of susceptible and protective HLA antigens for HT

*HLA-A*02:07*, *HLA-B*46:01*, *HLA-DRB1*08:03*, and *HLA-DRB4* were positively associated with HT, respectively ($Pc < .05$) (Table 1). Consistent with LD among *HLA* alleles, we observed that the association of *HLA-B*46:01* and *HLA-DRB1*08:03* with HT did not keep significance in the conditional analysis with adjustment for *HLA-A*02:07* (Supplemental Table 4). We identified *HLA-A*02:07* and *HLA-DRB4* as primary HT-susceptible antigens in this study.

*HLA-C*14:03*, *HLA-B*44:03*, *HLA-DRB1*13:02*, *HLA-DRB3*, *HLA-DQB1*06:04*, and *HLA-DPB1*04:01* showed significant effects against the development of HT ($Pc < .05$) (Table 1), and all of them were components of HP-2. Similar to GD cases, we could not pinpoint primarily associated antigens on HP-2 with conditional analysis due to strong LD (Supplemental Table 5), but a haplotype-based association study showed the significant protective association of HP-2 with HT (Supplemental Table 3).

Direct comparison of HLA antigen frequencies between GD and HT

In the direct comparison of the frequencies of HLA antigens between the diseases, we found that 2 HLA class II antigens, HLA-DR14 and HLA-DP5, were significantly increased in GD (Table 1). Other GD-susceptible antigens (HLA-B35 and HLA-B46) and HT-susceptible antigens (HLA-A2 and HLA-DR53) were not detected as specific antigens for either disease. This finding was explained by the observation that all these antigens were increased in either disease at least at the significance level of $P < .05$ (Table 1). Therefore, it is suggested that these 4 alleles are commonly susceptible to GD and HT. Similarly, with respect to the protective HLA antigens, there was no significant difference in the frequencies between GD and HT, and all of them were suggested to be protective against both diseases.

Epistatic interaction between protective and susceptible alleles in GD and HT

To detect the epistatic interaction between protective and susceptible HLA alleles, we divided the patients with GD into HLA-DP5–positive and –negative groups and analyzed the effect of protective HP-2 HLA alleles common to GD and HT. For HP-2, we arbitrarily used HLA-DR13 to represent this haplotype, which is located in the middle of HP-2. We found that the ORs of HLA-DR13 were significantly less than 1.0 in both groups (OR = 0.50, 95% CI = 0.30–0.83, $P = 7.0 \times 10^{-3}$ and OR = 0.12, 95% CI = 0.04–0.39, $P = 4.4 \times 10^{-4}$ in the HLA-DP5–positive and –negative groups, respectively) (Figure 1A). This